A new time-scale for ray-finned fish evolution

ELECTRONIC SUPPLEMENTARY MATERIAL

Imogen A. Hurley[1], Rachel Lockridge Mueller[1], Katherine A. Dunn[2], Eric J. Schmidt[1], Matt Friedman[4], Robert K. Ho[1,4], Victoria E. Prince[1,4], Ziheng Yang[3], Mark G. Thomas[3], and Michael I. Coates[1,4]

[1] *Department of Organismal Biology and Anatomy, University of Chicago, IL 60637, USA.*

[2] *Department of Biology, Dalhousie University, Halifax, NS, B3H 4J1, Canada.*

[3] *Department of Biology, University College London, Gower Street, London WC1E 6BT, UK.*

[4] *Committee on Evolutionary Biology, University of Chicago, IL 60637, USA.*

(a) ***Morphological material examined and other data sources***

Discoserra pectinodon: Carnegie Museum of Natural History CM 27290; CM 27295; CM 27333; CM 35211; CM 35214; CM 35217; CM 35547; CM 41009. *Brachydegma caelatum*: Museum of Comparative Zoology, Harvard University MCZ 6503 (holotype); MCZ 6504.

Morphological data for included taxa were also taken from the following references: *Acipenser* Grande & Bemis 1991, Hilton 2004; *Amia* Grande & Bemis 1998; *Amphicentrum* Coates 1988; *Australosomus* Nielsen 1949; *Caturus* Patterson 1975, Grande & Bemis 1998; *Dapedium* Patterson 1975, Thies 1989b, Thies & Herzog 1999; *Dipteronotus* Bürgin 1992; *Ebenaqua* Campbell & Le Duy Phuoc 1983; *Elops* Patterson 1973, 1975; *Hiodon* Hilton 2002; *Hulettia* Schaeffer & Patterson 1984; *Lepidotes* Patterson 1975, Thies 1989a, Cavin & Suteethorn 2006; *Lepisosteus* Mayhew 1924, Patterson 1975, Grande & Bemis 1998; *Luganoia* Bürgin 1992; *Macrepistius* Schaeffer 1960, 1971; *Macrosemius* Bartram 1977, González-Rodríguez *et al.* 2004; *Mesopoma* Coates 1993, 1999; *Mesturus* Nursall 1999, Nursall & Maisey 1991; *Mimia* Gardiner 1984; *Pachycormus* Mainwaring 1978, Lambers 1992; *Peltopleurus* Bürgin 1992; *Perleidus*: Patterson 1975, Burgin 1992; *Pholidophorus* Patterson 1973, 1975; *Polypterus* Bartsch & Gemballa 1992, Bartsch *et al*. 1997; *Pteronisculus* Nielsen 1942, Coates 1998; *Semionotus* Olsen & McCune 1991, Wenz 1999, Cavin & Suteethorn 2006; *Watsonulus* Olsen 1984, Grande & Bemis 1998.

All fossil taxa have been coded at genus level, so that certain taxa (e.g. *Lepidotes*) represent compound coding from two or more incompletely known species. Where genus monophyly is uncertain (e.g. *Pholidophorus*), data are drawn from references that address problems of taxon assignment.

(b) ***Morphological character set***

Other sources for discussions of similar or contrasting character formulations are identified as follows: [A] from Arratia 1999; [C] from Coates 1999; [CS] from Cavin & Suteethorn 2006; [GML] from Gardiner *et al.* 1996; [GS] from Gardiner & Schaeffer 1989, and Gardiner *et al*. 2005; [L] from Lund 2000; [OM] from Olsen & McCune 1991; [P] from Patterson 1982;

1. Opisthotic [CS].
   0. Present.
   1. Absent.
2. Opisthotic-pterotic relationship [GML].
   0. Opisthotic larger than pterotic.
   1. Opisthotic and pterotic subequal.
   Discoserra neurocranium (CM 27295A, B), shows opisthotic region not larger than pterotic. Code as 1.
3. Pterotic.
   0. Present.
   1. Absent.
4. Pterotic fused with dermopterotic. [GML].
   0. Absent.
   1. Present.
   Discoserra neurocranium lateral view from peels of CM 27295A, B, shows dermopterotic fused to pterotic. Code as 1.
5. Epioccipital.
   0. Present.
   1. Absent.
6. Epioccipital [GML].
   0. Epioccipital present bordered anteriorly by cranial fissure.
   1. Epioccipital contacts otic region.
   Discoserra neurocranium lateral aspect from peels of CM 27295A, B, shows no clear boundary of the epioccipital region, but it is fully ossified with no evidence of an open cranial fissure. As with *Dapedium* (Patterson 1975) it is likely that this bone extended into the otic region. Code as 1.
7. Intercalar [CS].
   0. Present.
   1. Absent.
8. Intercalar [GML].
   0. Endochondral with minor membranous outgrowths.
   1. With extensive membranous outgrowths medial to jugular (with or without endochondral core).
   2. With extensive membranous outgrowths lateral to jugular (with or without endochondral core).
   Discoserra neurocranium lateral view from peels of CM 27295A, B, shows a process in the intercalar region like that of *Perleidus* (Patterson 1975: fig. 115), lacking membranous outgrowths. Code as 0.

9. Vagal foramen [GML; CS].
   0. Anterior to exoccipital.
   1. lateral outgrowths from intercalar form posterior margin.
   2. Ventral outgrowths from intercalar lateral margin enclose dorsal margin.
   3. Enclosed by exoccipital.
   Discoserra neurocranium in lateral view from peels of CM 27295A, B, shows a large vagal foramen directed ventrally, resembling conditions in *Heterolepidotus* (Patterson 1975, fig. 103), but without indications of an intercalary with outgrowths. Code as 0.
10. Subtemporal fossa [GS].
   0. Absent.
   1. Present.
   Discoserra neurocranium in lateral view from peels of CM 27295A, B, shows a depressed area ventral to the hyoid facet and above the level of the jugular groove, consistent with Patterson's (1975) and Gardiner's (1984) observations of a subtemporal fossa position on the opisthotic. However, the condition in *Discoserra* is uncertain. Code as ?
11. Dilatator fossa [GS].
   0. Absent.
   1. Present.
   Discoserra neurocranium lateral view from peels of CM 27290 (supplementary figure 1a, dlf) and CM 27295A, B, shows a deep and faintly fluted dilatator fossa as present. Code as 1.
12. Posterior myodome [GS; GML; C; CS].
   0. Absent.
   1. Paired
   2. Intramural, lined by endoskeletal floor.
   3. With incompletely ossified (fenestrate) floor.
   Discoserra neurocranium from peels of CM 27295A, B, shows the large anterior opening of a median posterior myodome, the roof of which is pierced by a palatine foramen. Code as 2.
13. Anterior myodome [GML; C; CS; A].
   0. Absent
   1. Paired
   2. Through orbitonasal canal
   3. Median
   Discoserra neurocranium from peels of CM 27295A, B, shows an anterior myodome. Code as 1.
14. Cranial fissures [C].
   0. Otico-occipital (metotic) fissure present and separate from ventral cranial fissure, if present.
   1. Ventral otic and otico-occipital fissure confluent via vestibular fontanelle.
   2. Fissures non-persistent (closed), or pattern obscured by incomplete ossification.
   Discoserra neurocranium from peels of CM 27295A, B, shows no evidence of open fissures. Code as 2.
15. Hyoid facet [GS].
   0. Directed postero-ventrally.

1. Directed ventrally: facet horizontal.
Discoserra neurocranium from peels of CM 27295A, B, shows a horizontal hyoid facet; CM 27290 (supplementary figure 1a) displays the right side of the neurocranium with the hyomandibula preserved in-situ, with the anteroposteriorly broad head in articulation with the facet. Of the remainder of the hyomandibula, the foramen for the hyoid branch of n.VII lies in mid-shaft, with the opening directed ventrally. The rear of the hyomandibula is obscured by the operculum. Code as 1.

16. Basioccipital aortic canal [GML; C].
0. Present; in some examples bifurcates anteriorly.
1. Pronounced aortic groove.
2. Absent, shallow depression in ventral midline of basioccipital.
3. Parabasal canal between parasphenoid and basioccipital.

17. Foramina in basioccipital for occipital or spinal arteries.
0. Absent.
1. Present.
Discoserra aortic canal condition uncertain: in lateral aspect, the posterior plate of the parasphenoid bears an elongate anterolaterally directed groove that probably accommodated a lateral aorta, having diverged from its counterpart anterior to the occiput. The condition is most comparable to that in *Lepidotes* (Patterson 1975: fig. 109) and *Dapedium* (Patterson 1975), but location of ligament insertion is uncertain. Code as ?.

18. Lateral commissure breadth.
0. Anteroposteriorly broad.
1. Slender.
Schaeffer and Paterson (1984) identify this as a "holostean"-level feature of *Hulettia*; much the same condition is visible in *Discoserra*, CM 27290 (supplementary figure 1, lcm). Code as 1.

19. Posttemporal fossa / fossa bridgei [GS; GML; CS].
0. Posttemporal fossa absent, fossa bridgei rudimentary.
1. Posttemporal fossa small, fossa bridgei discrete.
2. Posttemporal fossa large, fossa bridgei discrete.
3. Posttemporal fossa communicates with fossa bridgei.
Discoserra neurocranium from peels of CM 27295A, B, shows a dorso-ventrally deep posterior opening to a posttemporal fossa (also visible on CM 27290, supplementary figure 2b, ptf), but continuity with the fossa bridgei is unknown. For detailed discussion of conditions, see Patterson 1975. Code as 2 & 3.

20. Spiracular canal [P; GS].
0. Absent.
1. Present.
Discoserra neurocranium from peels of CM 27295A, B, shows the postorbital process and lateral commissure as well preserved; absence of a groove indicates the presence of an enclosed tube communicating with the space housing a spiracular organ. There is no evidence of an external spiracular opening. Code as 1.

21. Spiracular canal within prootic.
0. Absent.
1. Present.

In most neopterygians the spiracular canal is located within the sphenotic, or the border between sphenotic and prootic - a likely condition for *Discoserra*. Schaeffer and Patterson (1984) noted the derived condition of *Hulettia* in which the canal is enclosed within the prootic, a condition otherwise known only in *Lepidotes*. For *Discoserra*, code as 0.

22. Basipterygoid process [GS; GML].
    0. Well developed dermal process with endoskeletal component.
    1. Basipterygoid process absent.
    Discoserra has a well-developed parasphenoid with 'no obvious palatal articulations' (Lund 2000: fig. 12). However, prominent basipterygoid processes are not well known in other deep-bodied early actinopterygians (e.g. *Platysomus*, Moy-Thomas & Bradly Dyne 1938). Code as 1.
23. Vomer sutured to parasphenoid.
    0. Separate from parasphenoid
    1. Sutured to parasphenoid.
    2. Vomer absent.
    The vomer has generally been considered paired in nonteleostean actinopterygians and single in most teleosts. This distinction is less clear now that paired and median vomers are known in *Dapedium* (Thies and Herzog 1999) and ontogenetic fusion occurs in *Hiodon* (Hilton 2002). From previous use of this character, the relation to the anterior of the parasphenoid is retained as a useful marker of a large sub-section of the neopterygian stem group. *Discoserra* vomers are unknown. Code as ?.
24. Parasphenoid: internal carotid foramen [GML].
    0. Absent.
    1. Present.
    Discoserra shows no clear evidence of a parasphenoid foramen for the internal carotid artery. Code as 0.
25. Parasphenoid: efferent pseudobranchial foramen [GML].
    0. Absent.
    1. Present.
    Discoserra neurocranium from peels of CM 27295A, B, shows a foramen in a likely position for the efferent pseudobranchial, but relation to parasphenoid or basisphenoid uncertain. Code as ?.
26. Dermopterotic [GS; C].
    0. Absent: separate supratemporal and intertemporal.
    1. Present.
    Brachydegma (figure 2c) has a large dermopterotic partly divided by a distinct slot into regions that Dunkle (1939) labeled supratemporal and intertemporal. Code as 1. For *Discoserra*, see note for dermosphenotic. Code as 1.
27. Dermosphenotic [GML].
    0. Hinged to skull roof.
    1. Bound or fused to anterior margin of sphenotic.
    The *Discoserra* skull roof interpretation used here (figure 2a, CM 35211B) differs from that presented by Lund (2000). A dermopterotic is coded as present because specimens of *Guildayichthys* and *Discoserra* show a canal-bearing bone attached firmly to and roofing the pterotic portion of the neurocranium. The

sphenotic/autosphenotic region in CM 27295A, B, retains part of the overlying dermal bone, a keystone shaped canal-bearing plate at the posterodorsal apex of the infraorbital series. This is interpreted as the dermosphenotic; it is not bound closely to, or fused with, the skull roof, and resembles the condition in *Lepisosteus* rather than *Amia*. Code as 0. The condition in *Brachydegma* is not clear. Code as ?.

28. Supraorbitals.
    0. Absent.
    1. Present.
    Discoserra has one or more supraorbitals; likewise *Brachydegma* (figures 2a, c, spo). Code as 1 for both genera.
29. Anterior supraorbitals meet infraorbitals [GML].
    0. Absent.
    1. Present.
    Discoserra lacks anterior supraorbital-infraorbital contact. Code as 0.
30. Anamestic suborbital series extends from anterior infraorbital to dorsal limit of preopercular stem.
    0. Absent.
    1. Present.

Series in *Discoserra* (figure 2a, sbo) matches conditions in *Lepidotes* and *Dapedium*. Code as 1.

31. Antorbital [GS; L].
    0. Absent.
    1. Present.
    2. Canal-bearing maxilla precludes identification of discrete antorbital.
    Discoserra has a large plate at the anterior of the infraorbital series, the antorbital or infraorbital identity of which is uncertain because the sensory canal pattern is unclear (a dorsally directed branch would indicate antorbital affinity). It is interpreted here as the anteriormost infraorbital (lachrymal) (figure 2a, la). Code as 0. *Brachydegma* (figure 2c, d) has a distinct antorbital, preserved best on the left side of the type, MCZ 6503, identified by Dunkle (1939) as infraorbital 4. Code as 1.
32. Antorbital shape.
    0. Platelike, with minimal (if any) distinct anterior process.
    1. Tapering towards slender anterior process; tri-radiate canal within broader, posterior, portion.
    2. Tubular.
    Brachydegma antorbital corresponds to conditions 0 or 1, with an incomplete anterior process (figure 2d, antpr). Code as 0 & 1. Pycnodont conditions are highly variable, and the exemplar taxon included in the present analysis, and the course of the sensory canals in the antorbital region of *Mesturus* is uncertain. Code as ?.
33. Infraorbitals anterior to circumorbital ring [OM; CS].
    0. Absent.
    1. Present.
    Discoserra lacks lachrymals anterior to the circumorbital ring (from peel of CM 35211B). Code as 0.
34. Rostral [GML; L].
    0. Cap on snout apex partially or wholly separating the nasals.

1. Of moderate to narrow size.
2. Reduced to a narrow tube with lateral processes.
3. A short tube.
4. Fused to something else (viz. rostrodermethmoid).
5. Mosaic of rostral bones.

Discoserra has a rostral plate separating the nasals completely. Although this is not a cap, as in *Perleidus* or *Australosomus*, it approximates to this condition more closely than alternatives, incompletely separating nasals (e.g. *Amia*). Code as 0. Similarly so for extant taxa such as *Hiodon*, in which a supraethmoid plate separates the nasals. In *Brachydegma* the rostral is small and tube-like, but the state of lateral processes is uncertain. Code as 2 & 3.

35. Premaxilla.
0. Present.
1. Absent.

36. Premaxilla ascending process [GS; GML; CS].
0. Absent.
1. Present, imperforate.
2. Present, grooved, notched and/or perforated.

Discoserra has a premaxilla with an elongate dorsal component flanking the rostral and extending to the base of the notch for the posterior nares (figure 2a, pmx). However, this bears dermal ornament and forms a roof to the olfactory region, unlike nasal processes in taxa such as macrosemiids, *Watsonulus*, semionotids and teleosts. Code as 0. Cavin and Suteethorn (2006) code for the presence of an ascending process that participates in the dermal skull roof cover as a possible synapomorphy of certain semionotids (*Pliodetes* Wenz 1999) and lepisosteids. This may be difficult to distinguish from plesiomorphic conditions. A characterization of nasal and antorbital overlap relative to the deep portion of the ascending process is likely to be more informative.

37. Premaxilla mobile [A; CS].
0. Absent.
1. Present.

38. Maxilla [GS; GML].
0. Fixed to cheek.
1. Free, with long curved medial process.
2. Free, with short medial process.
3. Absent.

In agreement with Lund (2000), in *Discoserra* the maxilla is not held to any other skull bones (figure 2a, mx). The medial surface is visible in disarticulated material (CM 35547A), and the most thickly ossified area is the anteroventral extremity, where there is a distinct, medially directed boss. A similar condition is present in *Peltopleurus* (Burgin 1992). Lund cites the presence of a slight anterior articular facet in CM 27290 (*Discoserra*). Code as 0 & 2. In *Brachydegma* the anterior part of the maxilla has a curved medial process (figure 2e, mpr) resembling that of *Amia*. Code as 1.

39. Maxillary shape [GML; L; CS].
0. Elongate, broad posteriorly, stretches well behind orbit.

1. Elongate, narrow, stretches well behind orbit.
2. Elongate, narrow, stretches well behind orbit, indented posteriorly.
3. Short, ends anterior to or below mid-orbit.
4. Very short, sliver of bone.
5. Approaches right-angled triangle with rounded corners.

Discoserra maxilla corresponds to state 3, but note that the maxilla is more elongate in *Guildayichthys*. Code as 3. *Brachydegma* has an indented posterior margin to the maxilla, well behind the orbit. There is a distinct, sub-semicircular area of ornament at the rear margin of the maxilla, present on both sides of the skull. This area might be a separate scale-bone (figure 2e, scb?), indicating a more strongly indented maxilla shape. Code as 2.

40. Supramaxilla [GS; GML; CS].
    0. Absent.
    1. Present.

    Discoserra has no supramaxilla; the absence of this 'superfluous-looking bone' is also noted for several early crown-group neopterygians: *Macrosemius*, *Acentrophorus* and *Hulettia* (Schaeffer & Patterson 1984). Code as 0. *Brachydegma* appears to have no separate supramaxilla and coding is 'absent'. However, the posterior, expanded portion of the maxilla has a smooth, unornamented band (figure 2e, smb) dividing upper from lower portions; it remains possible that this bone is a compound ossification. Code as 0.
41. Preoperculum [OM; L].
    0. With broad dorsal margin.
    1. With narrow ascending limb.
    2. Absent.

    Discoserra has a preoperculum with a narrow ascending limb (figure 2a, pop). Code as 1. *Brachydegma* shows a broad dorsal margin. Code as 0.
42. Preoperculum and maxilla [GS].
    0. In contact with palatoquadrate.
    1. Not in contact with palatoquadrate.

    Discoserra maxilla and preoperculum are separated from the palatoquadrate. Code as 1.
43. Quadratojugal [GML; CS].
    0. Platelike, lateral to quadrate.
    1. Splintlike, free along posterior border of quadrate.
    2. Fused to quadrate.
    3. Absent.

    Discoserra shows no evidence of a dermal plate clearly attributable to the quadratojugal. There is a large, quadrangular suborbital plate directly anterior to the base of the preoperculum (figure 2a) but this shows no particular relation to the underlying quadrate. Code as 3. In *Brachydegma*, a quadratojugal is present, matching states 0 and perhaps 2 (figure 2c, qj); Dunkle (1939) names this bone 'preopercular 2'. Code as 0 & 2.
44. Symplectic.
    0. Absent.
    1. Present.

45. Symplectic articulation [OM; GML; CS].
    0. Absent.
    1. On inner, medial surface, of quadrate.
    2. Behind quadrate, in loose contact with preoperculum posteriorly.
    3. Behind quadrate, with articular connection to lower jaw, may be bound to preoperculum by membrane bone.
    Discoserra has a symplectic (supplementary figure 1a, sym, CM 27290; Lund 2000, fig. 11): a slender bone directed anteriorly from the base of the hyomandibula towards the grooved rear of the quadrate, aligned with the rear margin of the metapterygoid. This symplectic lies on the lateral face of palate, and must have contacted the pre-operculum. However, there is no suggestion of fusion between these elements. Conditions resemble those of *Pholidophorus germanicus* and semionotids but in the absence of any quadratojugal. Terminology and homologies used here for hyoid arch components follow Patterson (1982) rather than Veran (1988), in which the posterior ceratohyal is identified as an interhyal, and thus the more widely distributed interhyal of actinopterygians is homologised as a symplectic. Code as 1. Conditions in *Lepisosteus* are highly derived (Patterson, 1973), with the symplectic remote from the quadrate, however other relations of the bone correspond most closely to state 2.
46. Quadrate with elongate posteroventral process [A; CS].
    0. Absent.
    1. Present.
47. Interoperculum [GS; OM; GML; CS].
    0. Absent.
    1. Present.
    Discoserra has an interoperculum (figure 2a, iop); Lund (2000) argues for 1-3 interopercular bones present in this position. Code as 1. *Brachydegma* appears to have no interoperculum. Code as 0.
48. Surangular in lower jaw [P; GS].
    0. Absent.
    1. Present.
    In most specimens of the lower jaw of *Discoserra* (and *Guildayichthys*) the likely surangular region is obscured. Code as ?. *Brachydegma* has a surangular. Code as 1,
49. Compound coronoid process [GS; C; L].
    0. Absent.
    1. Present.
    A compound coronoid process is present in *Discoserra* although incompletely known (figure 2a, cpr; surangular contribution uncertain). Code as 1. A large compound coronoid process is visible in *Brachydegma* (figure 2c, cpr). Code as 1.
50. Gulars [GML; C; L; A; CS]
    0. Present.
    1. Absent.
    Discoserra and *Brachydegma* show one or more gulars as present. Code as 0.
51. Median gular large.
    0. Absent.
    1. Present.
    Brachydegma has a large median gular (figure 2c, mgu). Code as 1.

52. Ceratohyal [GML].
    0. Proximal ceratohyal long, relatively straight - same depth posteriorly as distal element.
    1. Proximal ceratohyal long, gently curved with very small, distal element.
    2. Proximal ceratohyal short and deep posteriorly.
    3. Proximal ceratohyal very short, and open dorsally.
    4. Proximal ceratohyal with constricted shaft; hourglass shaped in lateral view.
    Discoserra has left and right, short, stout, hourglass shaped ceratohyals preserved in articulation with branchiostegal rays in CM 41009A, B, (also noted in Lund 2000 as Field Museum of Natural History specimen PF 10207). Code as 4.
53. Epibranchials [GS; GML].
    0. Slender.
    1. With uncinate processes.
54. Neural spines [GML].
    0. Paired.
    1. Median, unpaired pre-ural neural spines.
    Coding for this character follows the summary presented by Grande and Bemis (1991). Median neural spines in acipenserids and *Polypterus* form separately from the neural arch components, with which they may fuse secondarily. Therefore, these are regarded as supraneural spines. The *Discoserra* axial skeleton, of which complete vertebral series are preserved in specimens CM 41009 (supplementary figure 1b) and 35547A, shows vertebrae 1-17 bearing robust supraneural spines articulating with paired (clearly separated) neural arches and spines. In vertebra 20 and succeeding members, left and right neural arches may be fused across the arch apex, although spine halves remain separated. Vertebra 24 shows the spine fused with the base of a supraneural. From vertebra 25 onwards, there is no indication of articulation or fusion with supraneural spines, and the neural spines are single and median (supplementary figure 1b, c, pnem). The ural zone begins at around vertebra 30; therefore, there are around 3 or 4 unpaired, pre-ural neural spines. There is some resemblance to the condition in *Semionotus* (Olsen & McCune 1991). Code as 1.
55. Dorsal and anal fin ray supports [GS; OM].
    0. Ratio of rays to supports variable and greater than 2:1
    1. Ratio of rays to supports 1:1 (excluding the most anterior and posterior rays).
    2. Ratio of rays to supports 2:1.
    Discoserra dorsal and anal fins display a ratio of no more than 2:1 fin ray to basal (radial) ratio. Code as 2.
56. Fulcral scales [GML; L; CS].
    0. Basal and fringing fulcra present.
    1. Basal and fringing fulcra greatly enlarged.
    2. Fringing fulcra very reduced or absent.
    Discoserra has very fine fringing fulcra on the leading, ventral, edge of the caudal fin (CM 41009A; figure 2b, frf). Code as 2.
57. Caudal fin rays [GS].
    0. Terminate at caudal extremity of body axis.
    1. Extend beyond termination of body axis.
    Discoserra has a classic abbreviated heterocercal tail (figure 2b). Code as 1.

58. Uppermost hypaxial caudal rays [GML].
    0. Fin-rays successively shorter from bottom to top.
    1. A bundle of elongate fin-ray bases extending over several hypurals.
    2. Dorsal and ventral fin-ray bases symmetrical.
    3. Fin-ray one-to-one on hypurals.
    Discoserra has the same condition as *Semionotus* (Olsen & McCune 1991). Code as 0.
59. Caudal neural spines [GS].
    0. Paired.
    1. Median.
    Discoserra has median caudal neural spines (supplementary figure 1b, c, mcns). Code as 1.
60. Uroneurals [GML; A; CS].
    0. Absent.
    1. Present.
    Discoserra has no uroneurals. Code as 0.
61. Ridge scales [GML; CS].
    0. Absent.
    1. Present along dorsal margin (with posteriorly directed spines).
    2. Present along both dorsal and ventral margins.
    Discoserra has a distinctive and well developed series of dorsal ridge scales, each with a forward facing hook, very like those of pycnodonts (CM 41009A) (Nursall 1999) Code as 2.
62. Clavicle [GML; L].
    0. Large, caps anterior end of cleithrum.
    1. Toothed plates on postbranchial lamina of cleithrum.
    2. Clavicle reduced, often with single row of denticles.
    3. Serrated organ (with 12 or more ridges of denticles) lateral to cleithrum (*22*).
    4. Absent.
    Discoserra has no clavicle. Code as 4.
63. Endoskeletal shoulder ossification reduced to mesocoracoid arch [OM; CS].
    0. Absent.
    1. Present.
64. One or more accessory postcliethra present [A].
    0. Absent.
    1. Present.
    Additional postcleithra are widespread among crown Neopterygii, including derived members of the stem group. However, *Discoserra* shows no trace of additional postcleithra. Code as 0. In contrast, *Brachydegma* has an accessory postcleithrum situated directly above the pectoral fin insertion. Code as 1.
65. Lateral line canal.
    0. Caudal terminus directed dorsally into or towards axial lobe.
    1. Caudal terminus directed posteriorly towards or onto fin.
    In primitive actinopterygians the lateral line canal lies sub-parallel to the main body axis, and extends onto the caudal extremity of the tail. Although rarely well preserved in fossils, in living chondrosteans the canal can be followed at the base of

the caudal squamation, just proximal to the insertion of the fin rays, to this distal extremity of the tail. Hilton (2004) notes the caudal direction of the canal in *Mimia*. In *Lepisosteus*, *Amia*, and teleosts, the canal either terminates at or near to the caudal peduncle, or in certain cases extends on to the caudal fin. Bartram (1977) noted this condition in *Macrepistius*; Gardiner *et al.* (1996) discuss the extension of the canal onto the fin as a possible synapomorphy of amiids. *Discoserra*, like *Lepisosteus* and *Semionotus*, shows the caudal terminus of the lateral line scales (ossicles) directed towards the mid-point of the caudal fin (figure 2b, tlln). Code as 1.

66. Optic tectum larger than telencephalon [C].
    0. Absent.
    1. Present.
67. Hypophysis and enclosing recess in neurocranium [C].
    0. Projects posteroventrally.
    1. Projects ventrally or anteroventrally.
68. Cerebellar corpus [C].
    0. Divided bilaterally.
    1. Undivided.
69. Cerebellar corpus [C].
    0. Enters fourth ventricle.
    1. Arches above fourth ventricle.
70. Cerebellar corpus with median anteriorly projecting portion [C].
    0. Absent.
    1. Present.

(c) *Morphological data matrix*

Polypterus
0?101?1?0000?2000000010000000?00?0000000000000000000000002101002000?00000
Acipenser
0?10011?000012030001012000000?00?051??3?02?0000000100000000000000000000
Lepisosteus
1?10011?30100212100100100101101111020040111120011100001011100111101111
Amia
1?1001012013221210210110011 0?0110102012111313011101101121310030010111 1
Elops
1?0101023113021211300111010100120401111111311110100011121111040111111 1
Hiodon
1?0101023113121111300111110000?0000111011311111011?401121111040012?????
Perleidus
0000000001121 1?0100100100101001000000000000000?0100000010101000????????
Hulettia
000000000????0?111?11011110100100A0102301111201111041?1101?1?04?11?????
Macrosemius
1?0001??3??3?212????00101100?0121?020130112??0111102 1?1110100 2?11?????
Watsonulus
010?00000?131112111100100111101102020121013130111010?11111100001??????
Brachydegma
??????????????????????????1?1?01A0D???1200?B???01101????????????1??????
Caturus
1?1001012113121211 2??1100110?0110202012111313011101111111111003????????

Semionotus
1?10011?3?131?12?????0100101101l1?02013111112011110011111010121l1?????
Lepidotes
1?10011?3113?2?111D?10?00101111112020131111120l?11001111l??012?11?????
Dapedium
??0?100?01121210113??0111101011000010231l111C?11100 3?1101??024?1??????
Mesturus
010?100?0013101???3??0111100?11?05010230 01?1??01110 3?11?1?1024?0??????
Pachycormus
0100100?1113011111310111010 0?01B040101111131101110100110121104 01??????
Macrepistius
0101010121131 21??12??1?00111001?020?012111?1??1??0?1?1?11??004????????
Discoserra
0?0?0100B?12121??1D101?0?101010?00000B30113120 ?1004?12210102 4?01?????
Mimia
0000000000001000000000000000?00?0000000000000000000000000000000??????
Pteronisculus
0000000000021100000100?00000?0100000000000000000100000?000000000?10??0
Mesopoma
???????????21?0???0??????100?00?000000000000???010000??0000??00?0010000
Luganoia
????????????????1???????1??1?1002?04000B300?0???0?1002??1210??0??01?????
Dipteronotus
????????????????1??????1?0?1?1?00?00000B000?????0???????1010??1??00?????
Australosomus
0000000001123100100101?00100?00?0?0000000030000100?01?001???01?0?11???
Ebenaqua
??????????????????????????1?1000?001???5000????0?010A??0200??24?01?????
Amphicentrum
0?010?000?121200?0110????100?00?000000500030000000???0000??00?0??????
Peltopleurus
??????????????????????????100?00?00000B101?3???0?100????210??04?01?????
Pholidophorus
0101000001133111111100?1110100100 2001C1111311111100??1101111 0???1?????

'A' = (0/1); 'B' = (0/2); 'C' = (1/2); 'D' = (2/3); '?' = unknown character state or logical impossibility.

(d) ***Results of morphological phylogenetic analysis***

Summary of test results describing morphological support for Neopterygii, and relationships among fossil taxa exemplifying a range of early actinopterygian clades. All searches were conducted using PAUP* 4.0b10 (Swofford 1998).

(i) *recent actinopterygian interrelationships*

An exhaustive search of 41 informative characters for 6 extant taxa yielded 1 shortest tree of 64 steps; CI: 0.81; RI: 0.75; RC: 0.61. Topology: *Polypterus* (root) (*Acipenser* (*Lepisosteus* (*Amia* (*Elops, Hiodon*))). Decay/Bremer support for the neopterygian crown node is 12 extra steps, but for the halecostome node only 2 extra steps. The single shortest cladogram (length = 64) supports the conventional halecostome arrangement. The other possible arrangements of taxa within Neopterygii are more costly: placing

lepisosteids as the nearest relatives of teleosts to the exclusion of amiids requires 5 additional steps (length = 69), but reconstructing a topology consistent with Holostei is only 2 steps longer than the shortest cladogram (length = 66). The shortest tree supporting the "Ancient Fish Clade" *sensu stricto* is unparsimonious, requiring 80 steps.

(ii) *fossil and recent actinopterygian interrelationships*
Analysis of 29 taxa and 70 characters yielded 116 shortest trees of 234 steps; CI = 0.47; RI = 0.7; RC 0.33. The strict consensus of shortest tree topologies is shown in supplementary figure 2a. *Discoserra* is reconstructed as the immediate sister-group of crown Neopterygii. *Brachydegma* is placed at the base of the amiid stem. When characters are re-weighted (rescaled consistency index and retention index best fit options), a re-run analysis yields only 3 shortest trees (supplementary figure 2b). The only polytomy retained subtends *Pteronisculus* and *Mesopoma* and higher total-group neopterygians. One of these trees forms the basis of the phylogeny in figure 4.

(e) *Fossil calibrations for divergence date estimates using nuclear genetic and mitochondrial genomic data*

The most recently published references listing minimum divergence dates across the whole span of actinopterygian evolution are now over a decade old (Gardiner 1993, Patterson 1993). Phylogenies have changed, new taxa have been discovered, morphological descriptions have been revised, and stratigraphic correlations and date estimates of the geological column have been improved. In the present document, large-scale tree topologies supporting nodes of interest are taken from Coates (1999), Gardiner & Schaeffer (2005), Patterson & Rosen (1977), and Johnson & Patterson (1996). The summary set out below provides a series of conservative node-date minimum estimates using non-controversial fossil markers. Geologic dates are from Gradstein et al. (2004) and apply to the most recent (upper) boundary of any given subdivision of the (ICS) stratigraphic chart. In addition to being justified in the text below, the position of all calibration points is indicated in figure 13.

(i) *Actinopterygii.*
The actinopterygian-sarcopterygian divergence is minimally dated at 416 Mya. The earliest body fossils (meaning partly articulated rather than isolated scales or teeth) of convincing stem-group actinopterygians date from the Eifelian (mid-Devonian, 392 Mya), but the earliest sarcopterygians date from the uppermost Silurian (Pridoli; 416 Mya). The Silurian scale taxon *Andreolepis* is often attributed to the Actinopterygii (and used as such by Inoue et al. 2005) but is unreliable as a marker because it probably derives from a stem osteichthyan (Friedman & Blom in press; Friedman in press). Although it is known from articulated material, the putative Emsian (398 Mya) actinopterygian *Dialipina* (Schultze & Cumbaa 2001) is not used as a calibration point here because many of its 'actinopterygian-like' characters probably represent osteichthyan symplesiomorphies. This interpretation is supported by a recent cladistic analysis that places this genus below the split between Actinopterygii and Sarcopterygii, along the osteichthyan stem (Friedman in press).

For the analyses of mitochondrial sequence data, the age of the actinopterygian crown-group is minimally placed at 392 Mya on the basis of stem actinopterans, ('stegotrachelids'; members of Gardiner & Schaeffer's (1989) "*Moythomasia* group") known from the Givetian/Eifelian boundary (Gardiner 1993). As the nuclear sequences analysed here do not include polypterids, age estimates cannot incorporate calibration points for crown-group Acintopterygii.

(ii) *Actinopteri.*
Divergence of the actinopteran total-group from polypterids dates from 392 Mya, indicated by the presence of stem-actinopterans from the Givetian/Eifelian boundary (Gardiner 1993). Although the morphological analysis performed here places the Frasnian *Mimia* as the most basal stem neopterygian, we argue that this result is spurious and has arisen from a data set designed to resolve the interrelationships of taxa proximal to the neopterygian crown. Instead, we accept the conventional interpretation of *Mimia* as a stem actinopteran (Gardiner 1984; Gardiner & Schaeffer 1989; Coates 1999; Gardiner *et al*. 2005). Here we assign a minimum date of 345 Mya to the actinopteran crown node, based on the interpretation of the Tournasian (Dinely & Metcalf 1999) *Cosmoptychius* (Coates 1999) as the earliest stem-group neopterygian. For both data sets, a maximum age of 392 Mya is imposed on this node, based on the minimum age for the polypterid/actinopteran split (see previous section). This is the only maximum employed in this study.

(iii) *Chondrostei.*
The oldest crown-group chondrosteans, which include the living paddlefishes and sturgeons, date from at least 130 Mya, marked by the Lower Cretaceous (Hauterivian) paddlefish *Protosephurus* from the Jehol biota (Grande *et al.* 2002). This minimum date is used to calibrate age estimates derived from both nuclear and mitochondrial data sets.

(iv) *Neoptergyii.*
Crown-group Neopterygii dates from 245 Mya, indicated by a series of parasemionotids (stem-amiids, acknowledging the likely paraphyly of this group, Arratia (2004)) from the Olenekian (Gardiner 1993; Grande & Bemis 1998). The minimum node date estimate for crown neopterygians can be revised to 284 Mya (Artinskian/Sakmarian boundary) in light of the re-diagnosis of *Brachydegma* (Dunkle 1937). These markers and dates would also obtain for a node subtending the hypothesized "Ancient Fish Clade" (Inoue et al. 2005). Since the oldest crown-group neopterygians (parasemionotids, *Brachydegma*) are more closely related to *Amia* than any other living neopterygian (figure 2), the ages given here are used to calibrate the divergence of *Amia* from its sister group rather than the neopterygian crown node. In the case of the halecostome topology, the node calibrated reflects the divergence between *Amia* and teleosts, while it indicates the split between *Amia* and gars in the holostean arrangement.

(v) *Teleostei.*
Crown-group Teleostei dates from at least 151 Mya, as indicated by the stem-elopomorph *Elopsomolos* from the Kimmeridgian (Arratia 2000). In both the nuclear and mitochondrial data sets, this date is set as a minimum age for the last common ancestor

between elopomorphs and higher teleosts rather than the teleost crown node, which reflects the divergence of osteoglossomorphs from all other teleosts. We note that the phylogenetic position of *Elopsomolos* as an elopomorph is not well supported, however, it remains highly likely that this taxon will remain in the teleost crown. *Yambiana* (Osteoglossomorpha) provides the closest alternative calibration.

(vi) *Osteoglossomorpha.*
Crown-group osteoglossomorphs are marked by the stem-hiodontid *Yambiania* from the Lower Cretaceous (Guo-Qing & Wilson 1999), to which we apply a date of 136 Mya because this genus seems to be earlier than *Lycoptera*, the previously used clade marker (the age of which is probably Hauterivian-Barremian, following revised estimates from Davis et al. 2001), and which might fall outside the crown clade (Hilton 2003). This calibration can only be applied to the mitochondrial data set, which incorporates multiple osteoglossomorphs, including *Hiodon*, the sister group to all other living osteoglossomorphs (Hilton 2003).

(vii) *Otocephala*
Crown-group otocephalans date from 146 Mya, marked by the Tithonian stem-ostariophysan *Tischlingerichthys* (Arratia 1997, 1999). This date is used to establish a minimum for crown-group otocephala in the mitochondrial data set (last common ancestor of [*Crossostoma* + *Cyprinus*] and [*Engraulis* + *Sardinops*]), while it also defines a minimum age for the split between *Danio* and *Onychorhynchus* for analyses of nuclear sequence data.

(viii) *Acanthomorpha*
The acanthomorph crown node-date is pegged at 94 Mya by a suite of Cenomanian taxa (Patterson 1993; Tyler & Sorbini 1996). Stem-members of acanthomorph lineages represented in the mitochondrial (*Polymixia*) and nuclear (Tetraodontiformes) data sets are known from these deposits, indicating that this date is an appropriate minimum for this clade in both.

REFERENCES

Arratia, G. 1997. Basal teleosts and teleostean phylogeny. *Palaeo Ichthyologica* **7**, 1-168.

Arratia, G. 1999 The monophyly of Teleostei and stem-group teleosts. Consensus and disagreements. In *Mesozoic Fishes 2- Systematics and Fossil record* (ed. G. Arratia & H. –P. Schultze), pp. 265-334. München, Germany, Verlag Dr. Friedrich Pfeil.

Arratia, G. 2000 Remarkable teleostean fishes from the Late Jurassic of southern Germany and their phylogenetic relationships. *Mitt. Mus. Nat.kd., Berl., Geowiss. Reihe* **3,** 137-179.

Arratia, G. 2004. Mesozoic halecostomes and the early radiation of teleosts. In *Mesozoic Fishes 3- Systematics, Paleoenvironments and Biodiversity* (ed. G. Arratia & A. Tintori), pp. 279-315. München, Germany, Verlag Dr. Friedrich Pfeil.

Bartram, A. W. H. 1977 The Macrosemiidae, a Mesozoic family of holostean fishes. *Bull. Br. Mus. Nat. Hist. (Geol.)* **29**, 137-234.

Bartsch, P. & Gemballa, S. 1992 On the anatomy and development of the vertebral column and pterygiophores in *Polypterus senegalus* Cuvier, 1829 ("Pisces", Polypteriformes) *Zool. Jb.*, *Anat*. **122**, 497-529.

Bartsch. P., Gemballa, S. & Piotrowski, T. 1997 The embryonic and larval development of *Polypterus senegalus* Cuvier, 1829: its staging with reference to external and skeletal features, behaviour and locomotory habits. *Acta Zool.* (Stockholm) **78**, 309-328.

Bemis, W. E., Findeis, E. K. & Grande, L. 1997 An overview of Acipenseriformes. *Environ. Biol. Fishes* **48,** 25-71.

Bürgin, T. 1992 Basal Ray-finned Fishes (Osteichthyes; Actinopterygii) from the Middle Triassic of Monte San Giorgio (Canton Tessin, Switzerland). *Mémoires suisses de Paléontologie* **114**, 1-164.

Campbell, K. S. W. & Phuoc, L. D. 1983 A late Permian actinopterygian fish from Australia. *Palaeontology* **26**, 33-70.

Cavin, L. & Suteethorn, V. 2006 A new semionotiform (Actinopterygii, Neopterygii) from Upper Jurassic – Lower Cretaceous deposits of north-east Thailand, with comments on the relationships of semionotiforms. *Palaeontology* **49**, 339-353.

Coates, M. I. 1988 *A New Fauna of Namurian (Upper Carboniferous) Fish from Bearsden, Glasgow* Ph. D. Thesis, University of Newcastle Upon Tyne.

Coates, M. I. 1993 New actinopterygian fish from the Namurian Manse Burn formation of Bearsden, Scotland. *Palaeontology* **36**, 123-146.

Coates, M. I. 1998 Actinopterygians from the Namurian of Bearsden, Scotland, with comments on the early evolution of actinopterygian neurocrania. *Zool. J. Linn. Soc*. **122**, 27-59.

Coates, M. I. 1999 Endocranial preservation of a Carboniferous actinopterygian from Lancashire, UK, and the interrelationships of primitive actinopterygians. *Phil. Trans. R. Soc. Lond.* B, **354**, 435

Davis, G. A., Zheng, Y., Wang, C., Darby, B. J., Zhang, C., & George, G. 2001 Mesozoic tectonic evolution of the Yanshan fold and thrust belt, with emphasis on Hebei and Liaoning provinces, Northern China. *Geological Society of America, Memoir* **194**, 171-197.

Dinley, D. L. & Metcalfe, S. J. 1999 *Fossil Fishes of Great Britain*. Peterborough: Joint Nature Conservation Committee.

Dunkle, D. 1939 A new paleoniscid fish from the Texas Permian. *Am. J. Sci*. **237**, 262-274.

Dutheil, D. B. 1999 The first articulated fossil cladistian: *Serenoichthys kemkemensis*, gen. et sp.nov., from the Cretaceous of Morocco. *J. Vertebr. Paleontol.* **19,** 243-246.

Friedman, M. in press *Styloichthys* as the oldest coelacanth: implications for early osteichthyan interrelationships. *J. Syst. Palaeontol.*

Friedman, M. & Blom, H. In press. A new actinopterygian from the Famennian of East Greeland and the interrelationships of Devonian ray-finned fishes. *J. Paleontol.*

Gardiner, B. G. 1984 The relationships of the palaeoniscid fishes, a review based on new specimens of *Mimia* and *Moythomasia* from the Upper Devonian of Western Australia. *Bull. Br. Mus. Nat. Hist. (Geol.)* **37**, 173-428.

Gardiner, B. G. 1993 Osteichthyes: Basal Actinopterygians. In *Fossil Record II* (ed. M. J. Benton), pp. 611-619. London: Chapman and Hall.

Gardiner, B. G., Maisey, J. G., & Littlewood, D. T. J. 1996 In *Interrelationships of fishes,* (ed M. L. J. Stiassney, L. R. Parenti, & G. D. Johnson) pp. 117-146. San Diego, Academic Press.

Gardiner, B. G. & Schaeffer, B. 1989 Interrelationships of lower actinopterygian fishes. *Zool. J. Linn. Soc*. **97**, 135-187.

Gardiner, B. G., Schaeffer, B. & Masserie, J. A. 2005 A review of the lower actinopterygian phylogeny. *Zool. J. Linn. Soc*. **144**, 511-525.

González-Rodríguez, K., Applegate S. P., & Espinosa-Arrubarrena, L. 2004 A New World macrosemiid (Pisces: Neopterygii – Halecostomi) from the Albian ofMexico. *J. Vertebr. Paleontol.* **24**, 281-289.

Gradstein, F. M., Ogg, J. G. & Smith, A. G. 2004 *A geologic time scale.* Cambridge: Cambridge University Press.

Grande, L. & Bemis, W. E. 1991 Osteology and phylogenetic relationships of fossil and Recent paddlefishes (Polyodontidae) with comments on the interrelationships of Acipenseriformes. *J. Vertebr. Paleontol.* **11**, Suppl. 1. pp. 1-121.

Grande, L. & Bemis, W. E. 1998 A comprehensive phylogenetic study of amiid fishes (Amiidae) based on comparative skeletal anatomy. An empirical search for interconnected patterns of natural history. *J. Vertebr. Paleontol.* **18**, Suppl. 1. pp. 1-690.

Grande, L., Jan, F., Yambuto, Y. & Bemis, W. E. 2001 *Protopsephurus liui*, a well-preserved primitive paddlefish (Acipenseriformes: Polydontidae) from the Lower Cretaceous of China. *J. Vertebr. Paleontol.* **22**, 209-237.

Hilton, E. J. 2002 Osteology of the Extant North American Fishes of the genus *Hiodon* Lesueur, 1818 (Teleostei: Osteoglossomorpha: Hiodontiformes) *Fieldiana: Zoology, New Series* 100: 1-142.

Hilton, E. J 2003 Comparative Osteology and phylogenetic systematics of fossil and living bony-tongue fishes (Actinopterygii, Teleostei, Osteoglossomorpha). *Zool. J. Linn. Soc.* **137**, 1-100.

Hilton, E. J. 2004 The caudal skeleton of Acipenseriformes (Actinopterygii: Chondrostei): recent advances and new observations. In *Recent Advances in the Origin and Early Radiation of Vertebrates* (ed. G. Arratia, M. V. H. Wilson. & R. Cloutier) pp. 599-617. München Germany, Verlag Dr. Friedrich Pfeil.

Inoue, J. G., Miya, M., Venkatesh, B. & Nishida, M. 2005 The mitochondrial genome of Indonesian coelacanth *Latimeria menadoensis* (Sarcopterygii: Coelacanthiformes) and divergence time estimation between the two coelacanths. *Gene* **349**, 227–235

Lambers P. 1992. On the ichthyofauna of the Solnhofen Lithographic Limestone (Upper Jurassic, Germany). Ph.D Thesis. Rijksuniversiteit, Groningen.

Lauder, G. V. & Liem, K. F. 1983 The evolution and interrelationships of the actinopterygian fishes. *Bull. Mus. Comp. Zool.* **150,** 95-107.

Lund, R. 2000 The new actinopterygian order Guildayichthyiformes from the Lower Carboniferous of Montana (USA). *Geodiversitas* **22**, 171-206.

Mainwaring, A. J. 1978 Anatomical and systematic review of the Pachycormidae, a family of Mesozoic fossil fishes. Ph.D Thesis, University of London.

Mayhew, R. L. 1924. The skull of *Lepidosteus platostomus*. *J. Morph* **38**, 315-342.

Moy-Thomas, J. A. & Bradly Dyne, M. 1938 The actinopterygian fishes from the Lower Carboniferous of Glencarthol, Eskdale, Dumfriesshire. *Trans. R. Soc. Edinb*. **59**, 437-480.

Nelson, G. J. 1969 Gill arches and the phylogeny of fishes, with notes on the classification of vertebrates. *Bull. Amer. Mus. Natur. Hist*. **141**, 475-552.

Nielsen, E. 1942 Studies on Triassic fishes from East Greenland. 1. *Glaucolepis* and *Boreosomus*. *Palaeozool. Groenland.,* **1**, 1-403.

Nielsen, E. 1949 Studies on Triassic fishes from East Greenland. 2. *Australosomus* and *Birgeria*. *Palaeozool. Groenland.,* **3**, 1-309.

Nursall, J. R. 1999 The family Mesturidae and the skull of pycnodont fishes. In *Mesozoic Fishes 2- Systematics and Fossil record* (eds Arratia G., Schultze H. -P.) pp. 189-214. München, Germany, Verlag Dr. Friedrich Pfeil.

Nursall, J. R. & Maisey, J. G. 1991 *Neoproscinetes* In *Santana Fossils. An illustrated Atlas* (ed. Maisey J. G.) pp. 124-136. Neptune City, NJ, T.F.H. Publications Inc.

Olsen, P. E. 1984 The skull and pectoral girdle of the parasemionotid fish *Watsonulus eugnathoides* from the Early Triassic Sakemena Group of Madagascar with comments on the relationships of the holostean fishes. *J. Vertebr. Paleontol.* **4**, 481-499.

Olsen, P. E. & McCune, A. R. 1991 Morphology of the *Semionotus elegans* species group from the Early Jurassic part of the Newark Supergroup of eastern North America with comments on the Family Semionotidae (Neopterygii) *J. Vertebr. Paleontol.* **11**, 269-292.

Patterson, C. 1973 Interrelationships of holosteans. In *Interrelationships of fishes* (eds Greenwood, P. H., Miles, R. S., Patterson, C.) pp. 233-305. *Zool. J. Linn. Soc*. **53,** Suppl. 1.

Patterson, C. 1975 The braincase of pholidophorid and leptolepid fishes, with a review of the actinopterygian braincase. *Phil. Trans. R. Soc. Lond. B* **269**, 275-579.

Patterson C. 1982 Morphology and interrelationships of primitive actinopterygian fishes. *Am. Zool.* **22**, 241-259.

Patterson, C. 1993 Osteichthyes: Teleostei. In *The Fossil Record II* (ed. M. J. Benton), pp. 621-656. London: Chapman and Hall.

Romer, A. S. 1966 *Vertebrate Paleontology*. 3rd edn. Chicago: The University of Chicago Press.

Schaeffer, B. 1960. The Cretaceous Holostean Fish *Macrepistius*. *American Museum Novitates* **2011**: 1-18.

Schaeffer, B. 1971. The Braincase of the Holostean Fish *Macrepistius*, with comments on Neurocranial Ossification in the Actinopterygii. *American Museum Novitates* **2459**: 1-34.

Schaeffer, B & Patterson C. 1984 Jurassic fishes form western USA, with comments on Jurassic fish distribution. *American Museum Novitates*, **2796**, 1-86.

Schultze, H.-P. & Cumbaa, S. L. 2001 *Dialipina* and the characters of basal actinopterygians. In *Major Events in Early Vertebrate Evolution* (ed. P. E. Ahlberg) 315-332. London: Taylor & Francis.

Swofford D. L. 1998 *PAUP*: Phylogenetic Analysis Using Parsimony (*and Other Methods). Version 4.0b10.* Sunderland, MA, Sinauer Associates.

Thies, D. 1989a *Lepidotes gloriae*, sp. nov. (Actinopterygii: Semionotiformes) from the Late Jurassic of Cuba. *J. Vertebr. Paleontol.* **9**, 18-40.
Thies, D. 1989b Der hirnschadel und das gehirn von *Tetragonolepis semicincta* Bronn 1830 (Actinopterygii, Semionotiformes) *Palaeontographica* Abt. A **209**, 1-32.
Thies D. & Herzog A. 1999 New information on *Dapedium* Leach 1822 (Actinopterygii, Semionotiformes) In *Mesozoic Fishes 2- Systematics and Fossil record* (eds Arratia G., Schultze H. -P.) pp. 143-152. München, Germany, Verlag Dr. Friedrich Pfeil.
Tyler J. C. & Sorbini, L. 1996 New superfamily and three new families of tetraodontiform fishes from the Upper Cretaceous: the earliest and most morphologically primitive plectognaths. *Smithsonian Cont. Palaeo.* **82,** 1-59.
Veran M. 1988 Les elements accessories de l'arc hyoidien des poisons téléostomes (Acanthodiens et Osteichthyens) fossils et actuels. *Memoires du Muséum National D'histoire Naturelle; Sciences de la Terre* **54**, 1-98.
Wenz S. 1999 *Pliodetes nigeriensis* gen. et sp. nov., a new semionotid fish from the Lower Cretaceous of Gadoufaoua (Niger Republic). In *Mesozoic Fishes 2- Systematics and Fossil record* (eds Arratia G., Schultze H. -P.) pp. 107-120. München, Germany, Verlag Dr. Friedrich Pfeil.
Zhu, M. & Schultze, H.-P. 1997 The oldest sarcopterygian fish. *Lethaia* **30**, 293-304.

Supplementary table 1. GenBank accession numbers for nuclear gene sequences used in this study. Numbers with asterisks were sequenced in this study. Numbers in bold were used in the concatenated data set.

Taxon	***fzd8***	***hoxa11***	***sox11***	***tyr***
Acipenser baerii	**AY333968**	-	**AY333969**	**AY333970**
Polyodon spathula	**DQ307742***	**Pers. com. R. Dahn**	**DQ307752***	**DQ307749***
Lepisosteus platyrhynchus	**AY333980**	-	**AY333981**	**AY333982**
Lepisosteus osseus	-	**DQ307746***	-	-
Amia calva FMNH *Amia* 1-05	**DQ307740P***	**DQ307745***	**DQ307750***	**DQ307747***
Arapaima gigas	-	-	AY333972	-
Gnathonemus petersii	AY333976	-	AY333977 **AY333978**	**AY333979**
Hiodon alosoides USNM 384559	DQ307741*	DQ307743* DQ307744*	DQ307751*	DQ307748*
Elops hawaiiensis	AY333973	-	**AY333974**	**AY333975**
Danio rerio	**AF060697 AF060696**	**AF071240 AF287137**	**NM_131336 NM_131337**	**AF542067**
Danio aequipinnatus	AF287136	-	-	-
Ictalurus punctatus	-	-	-	AF216388
Oncorhynchus mykiss	-	**AY567792** AY567793	**AB010741**	AB122031
Oryzias latipes	-	-	-	D29687
Takifugu rubripes+	**GENSCAN00000027025 GENSCAN00000019511**	**SINFRUG00000157392 SINFRUG00000138060**	**GENSCAN00000022722**	**GENSCAN00000018532 SINFRUG00000132700**
*Tetraodon nigroviridis^*	**GSTENG00015228001 GSTENG00016595001**	**HOXA11 HOXAb11**	**GSTENG00032152001**	**GSTENT00018906001**
Oreochromis niloticus	**AY333986**	**AY757320**	**AY333983**	**AY333984 AY333985**
Amphilophus citrinellum	-	-	AY333971	-
Xenopus laevis	**AF033110** AF017177	**AF287140**	**D86076** D87209	**AY333967**
Rana nigromaculata	-	-	-	D12514
Trionyx sinensis	-	-	-	S56789
Gallus gallus	-	NM_204619	AB012237	D88349
Coturnix japonicus	-	-	-	AB024278

Homo sapiens	**NM_031866**	**NM_005523**	**U23752**	**M27160**
Mus musculus	**NM_008058**	**NM_010450**	**NM_009234**	**D00440**
Rattus norvegicus	-	XM_575479	NM_053349	-
Bos taurus	-	-	-	AF445639
Canis familiaris	-	-	-	AY336053
Heterodontus francisci	-	**AF479755**	-	-

+ Ensembl Fugu v2.0 July 2005. ^Ensembl Tetraodon v7 July 2005.

Supplementary table 2. GenBank accession numbers for mitochondrial genomic sequences used in this study. Taxa with asterisks were sequenced in this study.

Taxon	Accession number	Taxon	Accession number
Scyliorhinus canicula	Y16067	*Osteoglossum bicirrhosum*	AB043025
Mustelus manazo	AB015962	*Pantodon bucholzi*	AB043068
Polypterus ornatipinnis	U62532	*Hiodon alosoides*	AP004356
Polypterus senegalus	AP004352	*Notacanthus chemnitzi*	AP002975
Erpetoichthys calabaricus	AP004350	*Anguilla japonica*	AB038556
Erpetoichthys calabaricus *	AY442348	*Gymnothorax kidako*	AP002976
Acipenser transmontanus	AB042837	*Conger myriaster*	AB038381
Scaphyrhynchus albus	AP004354	*Engraulis japonicus*	AB040676
Huso huso *	AY442351	*Sardinops melanostictus*	AB032554
Polyodon spathula	AP004353	*Cyprinus carpio*	X61010
Polyodon spathula *	AY442349	*Crossostoma lacustre*	M91245
Lepisosteus oculatus	AB042861	*Coregonus lavaretus*	AB034824
Lepisosteus oculatus *	AY442350	*Salmo salar*	U12143
Atractosteus spatula	AP004355	*Oncorhynchus mykiss*	L29771
Amia calva	AB042952	*Chlorophthalmus agassizi*	AP002918
Amia calva *	AY442347	*Polymixia japonica*	AB034826
		Pagrus major	AP002949

Supplementary table 3. Nuclear Divergence Date Estimates. Nuclear Bayesian divergence date estimates for key nodes in the actinopterygian phylogeny (halecostome topology, figure 3). No upper bound was placed on any node except for the Actinopteri (see supplementary figure 13).

Node	**Date (Myr ago)**	**Lower 95% Credibility Interval**	**Upper 95% Credibility Interval**
Elops b / *Gnathonemus* b	186	144	234
Takifugu b / *Tetraodon* b	50	28	81
Oreochromis b / [*Takifugu* b + *Tetraodon* b]	109	67	160
Danio b / *Onychorhynchus* b	170	147	213
[*Danio* b + *Onychorhynchus* b] / *Oreochromis* b [*Takifugu* b + *Tetraodon* b]	193	157	240
[*Elops* b + *Gnathonemus* b] / [*Danio* b + *Onychorhynchus* b] [*Oreochromis* b [*Takifugu* b + *Tetraodon* b]]	219	181	265
Takifugu a / *Tetraodon* a	37	15	65
Oreochromis a / [*Takifugu* a + *Tetraodon* a]	108	94	138
Danio a / *Oreochromis* a [*Takifugu* a + *Tetraodon* a]	246	206	292
Whole Genome Duplication Event	269	226	316
Halecostomi	311	266	358
Neopterygii	325	279	371
Acipenser / *Polyodon*	142	130	171
Actinopteri	372	347	391

Supplementary table 4. Nuclear Divergence Date Estimates. Nuclear Bayesian divergence date estimates for key nodes in the actinopterygian phylogeny (halecostome topology, figure 3). No upper bound was placed on any node except for the Actinopteri and including the newly diagnosed *Brachydegma* divergence dates (see supplementary figure 13).

Node	**Date (Myr ago)**	**Lower 95% Credibility Interval**	**Upper 95% Credibility Interval**
Elops b / *Gnathonemus* b	188	146	235
Takifugu b / *Tetraodon* b	51	29	82
Oreochromis b / [*Takifugu* b + *Tetraodon* b]	110	69	161
Danio b / *Onychorhynchus* b	172	147	217

[*Danio* b + *Onychorhynchus* b] / *Oreochromis* b [*Takifugu* b + *Tetraodon* b]	195	158	241
[*Elops* b + *Gnathonemus* b] / [*Danio* b + *Onychorhynchus* b] [*Oreochromis* b [*Takifugu* b + *Tetraodon* b]]	222	185	267
Takifugu a / *Tetraodon* a	37	15	67
Oreochromis a / [*Takifugu* a + *Tetraodon* a]	108	94	139
Danio a / *Oreochromis* a [*Takifugu* a + *Tetraodon* a]	250	213	294
Whole Genome Duplication Event	273	237	317
Halecostomi	317	287	359
Neopterygii	330	295	372
Acipenser / *Polyodon*	142	130	169
Actinopteri	373	348	391

Supplementary table 5. Nuclear Divergence Date Estimates. Nuclear Bayesian divergence date estimates for key nodes in the actinopterygian phylogeny (holostean topology). No upper bound was placed on any node except for the Actinopteri (see supplementary figure 13).

Node	**Date (Myr ago)**	**Lower 95% Credibility Interval**	**Upper 95% Credibility Interval**
Elops b / *Gnathonemus* b	187	147	233
Takifugu b / *Tetraodon* b	50	28	80
Oreochromis b / [*Takifugu* b + *Tetraodon* b]	106	66	155
Danio b / *Onychorhynchus* b	170	147	212
[*Danio* b + *Onychorhynchus* b] / *Oreochromis* b [*Takifugu* b + *Tetraodon* b]	193	157	236
[*Elops* b + *Gnathonemus* b] / [*Danio* b + *Onychorhynchus* b] [*Oreochromis* b [*Takifugu* b + *Tetraodon* b]]	217	181	262
Takifugu a / *Tetraodon* a	37	15	65
Oreochromis a / [*Takifugu* a + *Tetraodon* a]	107	94	136
Danio a / *Oreochromis* a [*Takifugu* a + *Tetraodon* a]	244	207	285
Whole Genome Duplication Event	264	227	306
Halecostomi	289	249	342

Neopterygii	324	284	368
Acipenser / *Polyodon*	142	130	170
Actinopteri	373	348	391

Supplementary table 6. Results of Kishino-Hasegawa (KH) and Shimodara-Hasegawa (SH) tests on morphological hypotheses of relationships for Acipenseriformes, Lepisosteidae, *Amia*, and Teleostei using mitochondrial genomic sequences.

Hypothesis of relationship	-ln	KH	SH
(Acipenseriformes (Lepisosteidae (*Amia* + Teleostei)))[a]	61730.47	0.270	0.307
(Acipenseriformes ((*Amia* + Lepisosteidae) Teleostei)))[b]	61726.43	0.335	0.539
(Acipenseriformes ((*Amia* (Lepisosteidae + Teleostei)))[c]	61734.74	0.17	0.19

[a] Patterson, 1973; Lauder and Leim, 1983; Gardiner et al., 1996; Bemis et al., 1997; Coates 1999

[b] Romer, 1966; Nelson 1969

[c] Olsen, 1984

Supplementary table 7. Mitochondrial Divergence Dates. Mitochondrial Bayesian divergence date estimates for key nodes in the actinopterygian phylogeny (halecostome topology). No upper bound was placed on any node except for the Actinopteri (see figure 13).

Node	**Date (Myr ago)**	**Lower 95% Credibility Interval**	**Upper 95% Credibility Interval**
Polypterus	59	41	82
Erpetoichthys	7	4	12
Erpetoichthys/Polypterus	90	69	117
Lepisosteus	2	0.09	5
Atractosteus/Lepisosteus	78	55	110
Osteoglossidae/Pantodontidae	188	156	221
Osteoglossomorpha	251	220	283
Engraulidae/Clupidae	128	100	160
Baflitoridae/Cyprinidae	156	124	190
Otocephala	223	191	255
Oncorhynchus/*Salmo*	68	46	94
Coregoninae/Salmoninae	106	77	138
Pagrus/*Polymixia*	154	124	186
Neoteleostei	182	150	214
Euteleostei	212	180	244
Clupeocephala	255	224	286

Anguillidae/Congridae	164	134	193
Muraenidae/ Anguillidae+Congridae	181	151	212
Notacanthus/Anguilliformes	240	209	273
Elopocephala	285	256	315
Teleostei	296	268	326
Amia/*Amia*	14	6	31
Halecostomi	344	319	371
Neopterygii	351	327	378
Polyodon/*Polyodon*	15	3	39
Acipenser/Huso	75	47	110
Scaphirhynchinae/Acipenserinae	127	89	170
Acipenseridae/Polyodontidae	226	185	265
Actinopteri	367	346	390
Actinopterygii	433	398	479

Supplementary table 8. Mitochondrial Divergence Dates. Mitochondrial Bayesian divergence date estimates for key nodes in the actinopterygian phylogeny (halecostome topology). No upper bound was placed on any node except for the Actinopteri and including the newly diagnosed *Brachydegma* divergence dates (see figure 13).

Node	**Date (Myr ago)**	**Lower 95% Credibility Interval**	**Upper 95% Credibility Interval**
Polypterus	59	41	81
Erpetoichthys	7	4	12
Erpetoichthys/Polypterus	90	68	116
Lepisosteus	2	0.08	5
Atractosteus/Lepisosteus	78	55	110
Osteoglossidae/Pantodontidae	188	157	221
Osteoglossomorpha	251	221	283
Engraulidae/Clupidae	128	100	159
Baflitoridae/Cyprinidae	155	124	189
Otocephala	223	192	255
Oncorhynchus/*Salmo*	68	47	94
Coregoninae/Salmoninae	106	78	137
Pagrus/*Polymixia*	154	125	186
Neoteleostei	182	151	214
Euteleostei	212	182	244
Clupeocephala	255	226	286
Anguillidae/Congridae	163	134	193
Muraenidae/ Anguillidae+Congridae	181	151	212
Notacanthus/Anguilliformes	240	210	272
Elopocephala	285	257	315
Teleostei	296	268	326

Amia/*Amia*	14	6	31
Halecostomi	344	319	372
Neopterygii	351	327	378
Polyodon/*Polyodon*	15	2	38
Acipenser/Huso	74	47	109
Scaphirhynchinae/Acipenserinae	126	89	168
Acipenseridae/Polyodontidae	225	185	265
Actinopteri	367	346	391
Actinopterygii	433	397	478

Supplementary table 9. Mitochondrial Divergence Dates. Mitochondrial Bayesian divergence date estimates for key nodes in the actinopterygian phylogeny (holostean topology). No upper bound was placed on any node except for the Actinopteri (see figure 13).

Node	**Date (Myr ago)**	**Lower 95% Credibility Interval**	**Upper 95% Credibility Interval**
Polypterus	59	41	81
Erpetoichthys	7	4	12
Erpetoichthys/Polypterus	90	68	117
Osteoglossidae/Pantodontidae	190	159	223
Osteoglossomorpha	254	223	286
Engraulidae/Clupidae	128	99	159
Baflitoridae/Cyprinidae	157	125	189
Otocephala	225	193	257
Oncorhynchus/Salmo	67	46	93
Coregoninae/Salmoninae	105	78	135
Pagrus/Polymixia	154	125	185
Neoteleostei	182	152	215
Euteleostei	213	182	244
Clupeocephala	258	227	289
Anguillidae/Congridae	166	136	197
Muraenidae/ Anguillidae+Congridae	183	152	216
Notacanthus/Anguilliformes	243	212	275
Elopocephala	288	259	318
Teleostei	300	271	329
Lepisosteus	1	0.09	4
Atractosteus/Lepisosteus	69	49	95
Amia/Amia	13	5	27
Holostei	328	299	358
Neopterygii	349	324	377
Polyodon/Polyodon	13	2	36
Acipenser/Huso	70	44	105

Scaphirhynchinae/Acipenserinae	120	83	163
Acipenseridae/Polyodontidae	217	176	257
Actinopteri	367	346	390
Actinopterygii	436	398	483

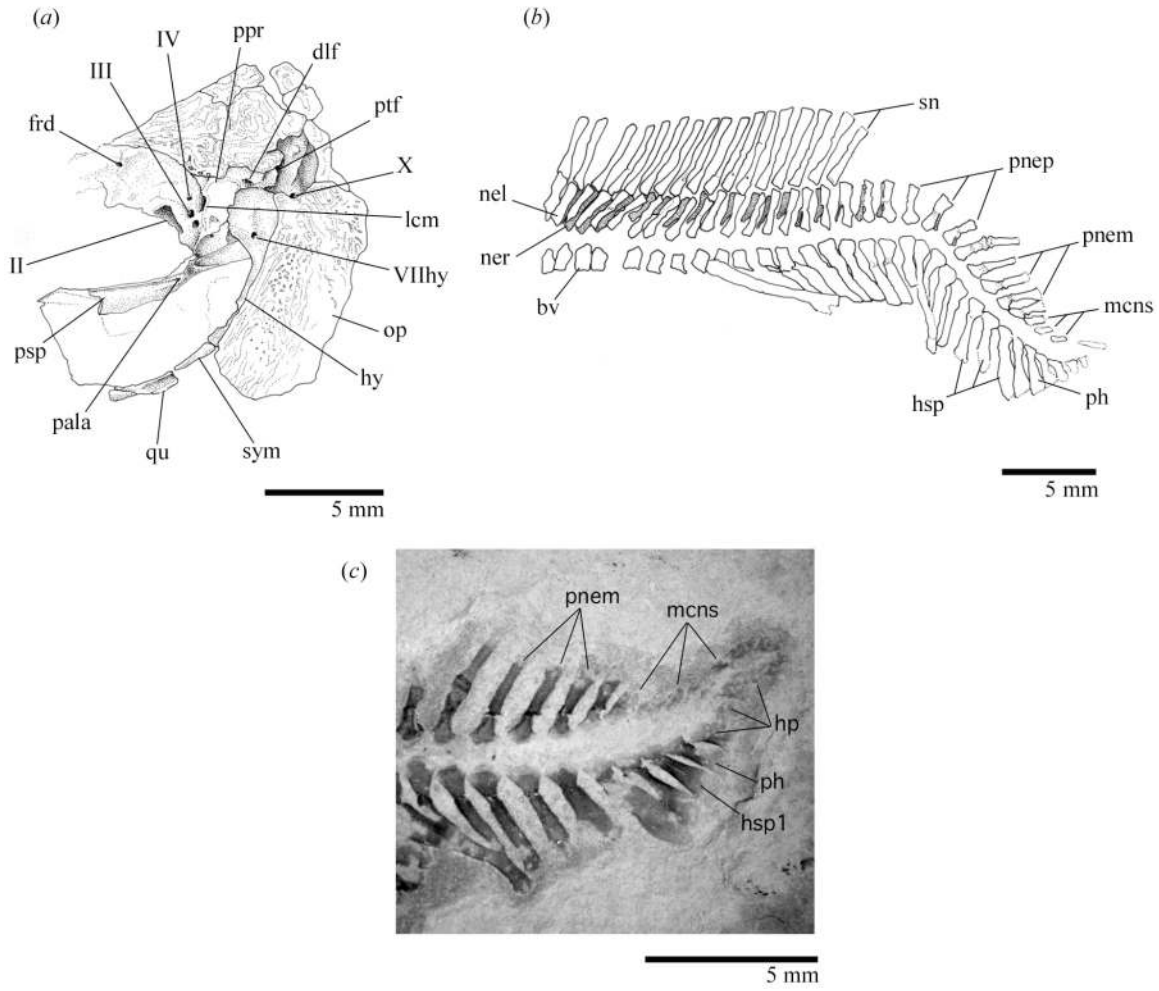

Supplementary figure 1. *Discoserra pectinodon* Lund (2000), an advanced stem-group neopterygian from the Mississippian (Serpukhovian) of Montana. All specimens shown in lateral view, anterior to left. Scale bars = 5mm. (a) Neurocranium, incomplete palate, and hyoid arch (CM 27290). (b) Axial skeleton (CM 35547A). (c) Caudal fin, internal skeleton (CM 35547A). Abbreviations are as follows: CM, Carnegie Museum of Natural History, Pittsburgh; bv, basiventral; dlf, dilatator fossa; frd, foramen for ascending branch of superficial ophthalmic nerve; hp, hypurals; hsp, haemal spines; hy, hyomandibula; lcm, lateral commissure; mcns, median caudal neural spines; nel, neural arch left; ner, neural arch right; op, opercular; pala, canal for anterior branch of palatine nerve; ph, parhypural; pnem, preural neural arch, median; pnep, preural neural arch, paired; ppr, postorbital process; psp, parasphenoid; ptf, posttemporal fossa; qu,quadrate; sn, supraneural; sym, symplectic; II, optic fenestra; III, foramen for oculomotor nerve; IV, foramen for trochlear nerve; VIIhy, foramen for hyoid branch of facial nerve; X, foramen for vagus nerve.

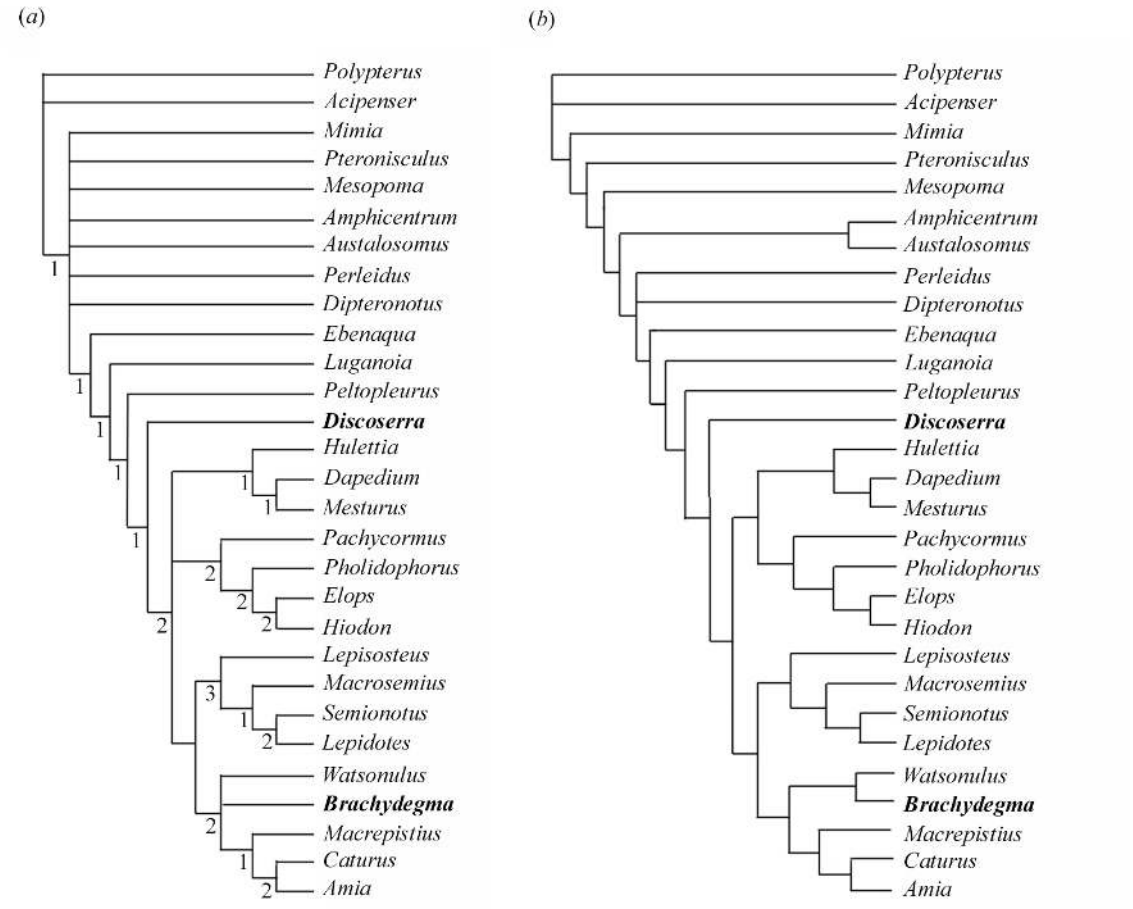

Supplementary figure 2. Cladograms derived from parsimony analysis of morphological data set. (a) Strict consensus of 116 trees. (b) Strict consensus of three trees after reweighting. Methods listed in main body of text.

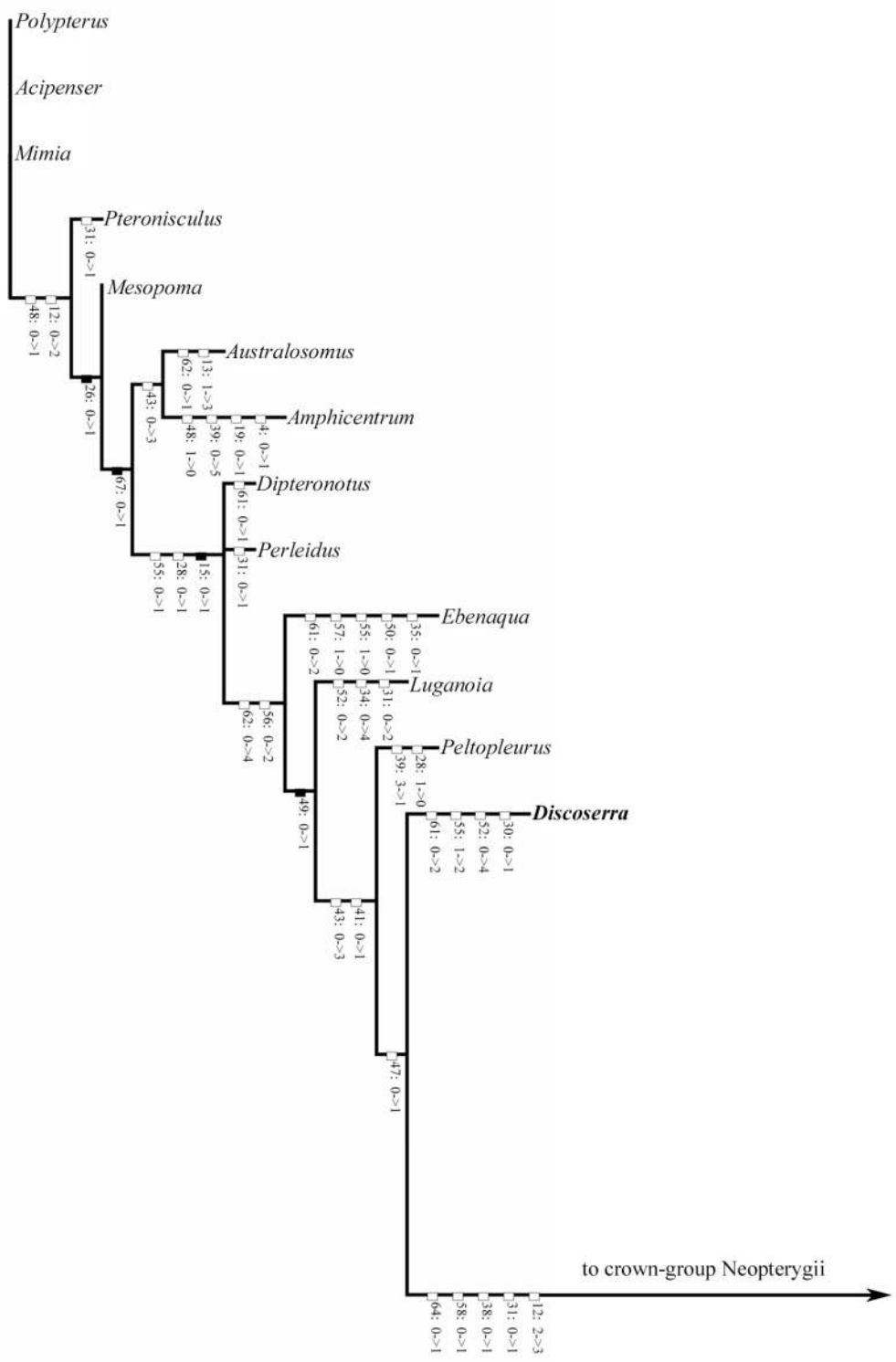

Supplementary figure 3. Unambiguous character changes plotted on one of the 116 shortest trees (L = 234; CI = 0.47; RI = 0.70; RCI = 0.33) recovered from maximum parsimony analysis of the morphological data set with all characters assigned equal weight. Character changes indicated with hollow boxes are homplastic, while those with solid boxes are unique. Continued in figure 4.

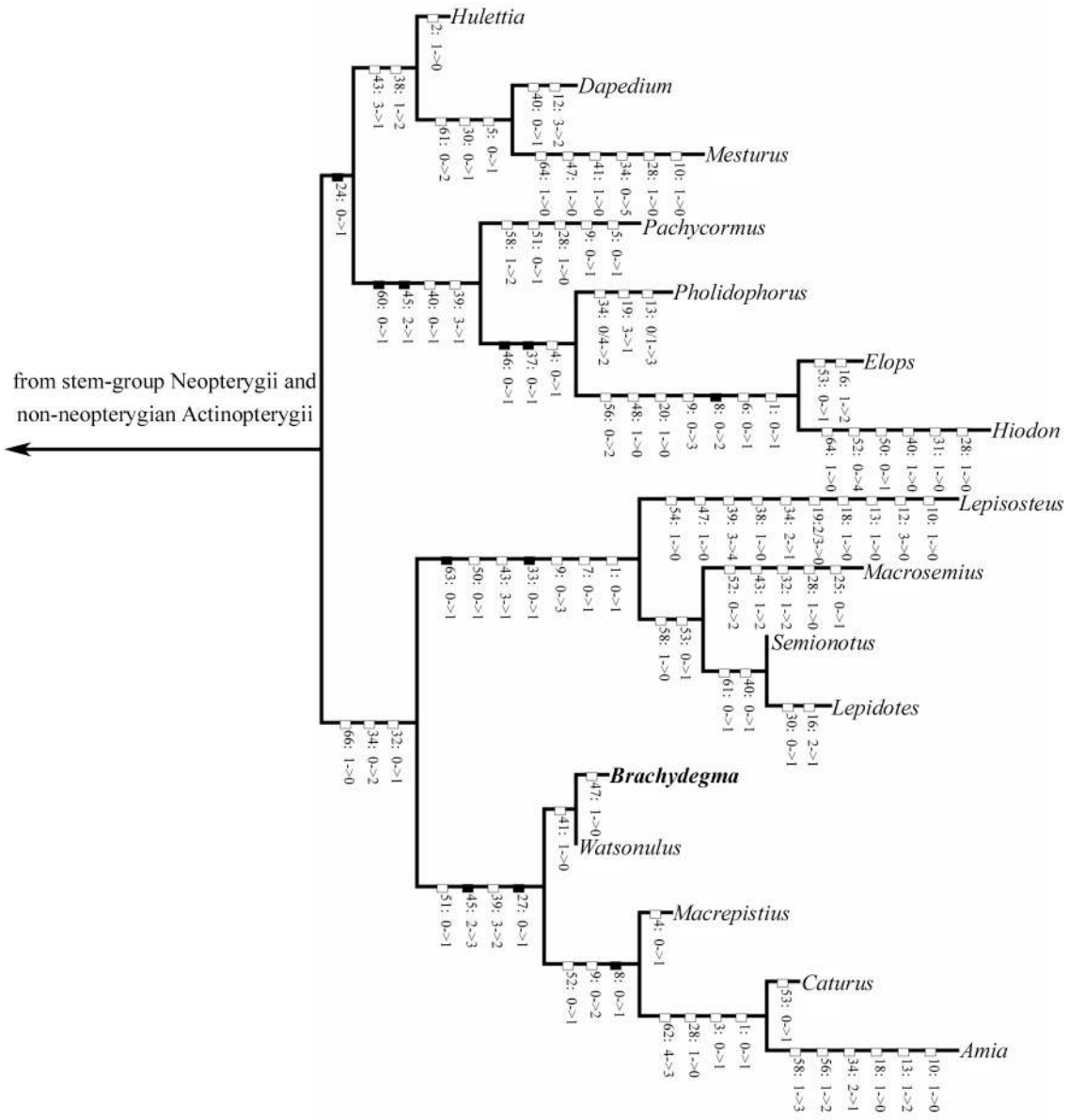

Supplementary figure 4. Unambiguous character changes plotted on one of the 116 shortest trees (L = 234; CI = 0.47; RI = 0.70; RCI = 0.33) recovered from maximum parsimony analysis of the morphological data set with all characters assigned equal weight. Character changes indicated with hollow boxes are homplastic, while those with solid boxes are unique. Continued from figure 3.

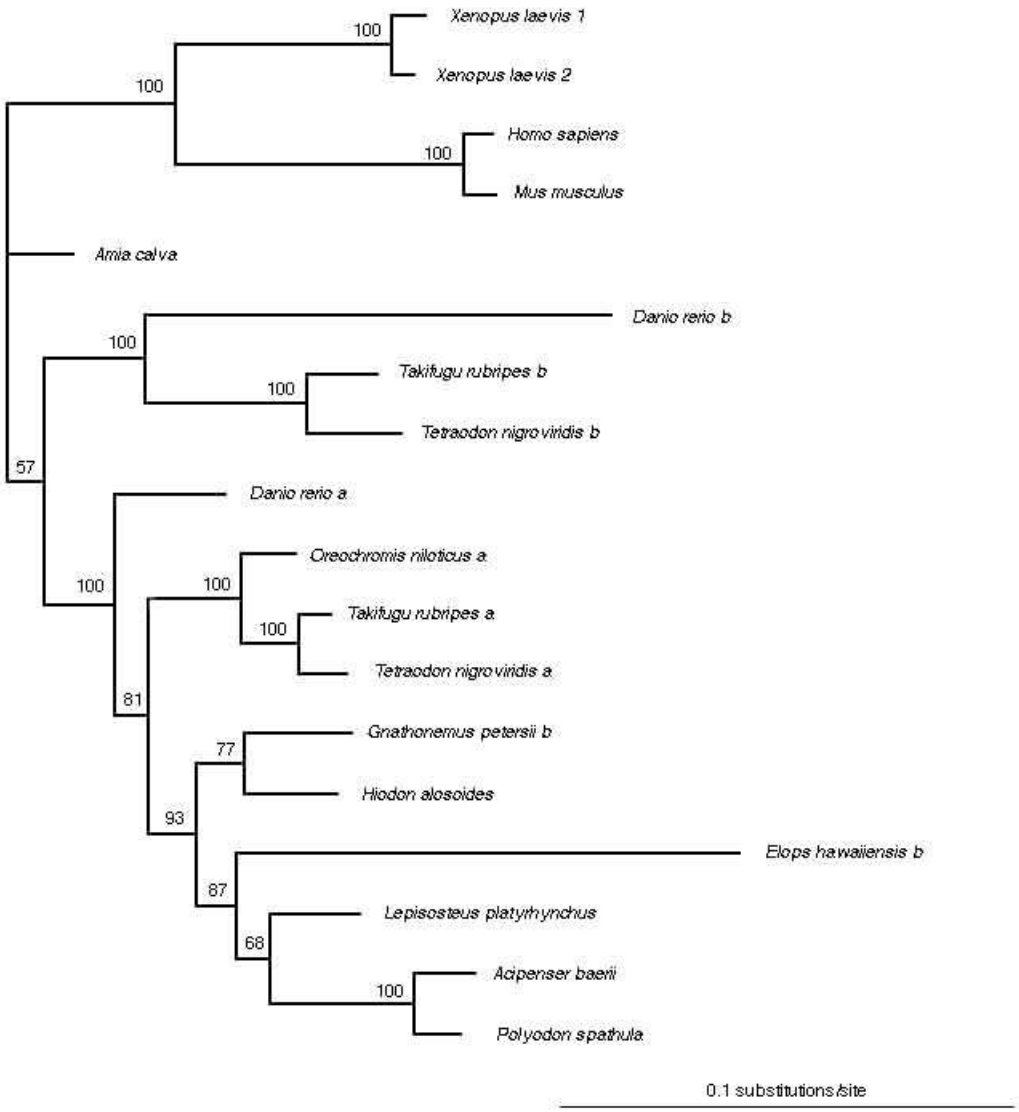

Supplementary figure 5. Bayesian tree derived from nucleotide sequences of nuclear gene data of first and second codon positions of *fzd8*. The SYM+I+Γ model of sequence evolution was used. The values above the branches indicate Bayesian posterior probabilities.

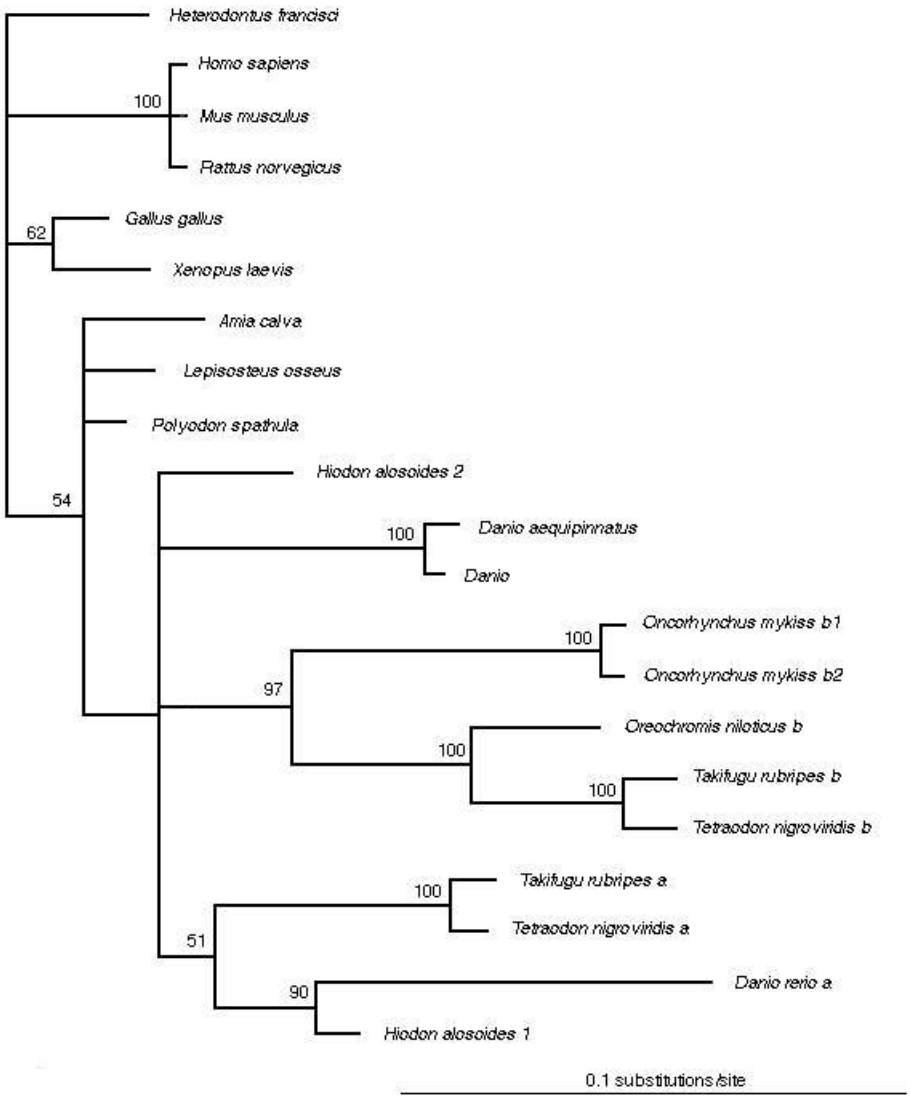

Supplementary figure 6. Bayesian tree derived from nucleotide sequences of nuclear gene data of first and second codon positions of *hoxa11*. The GTR+I model of sequence evolution was used. The values above the branches indicate Bayesian posterior probabilities.

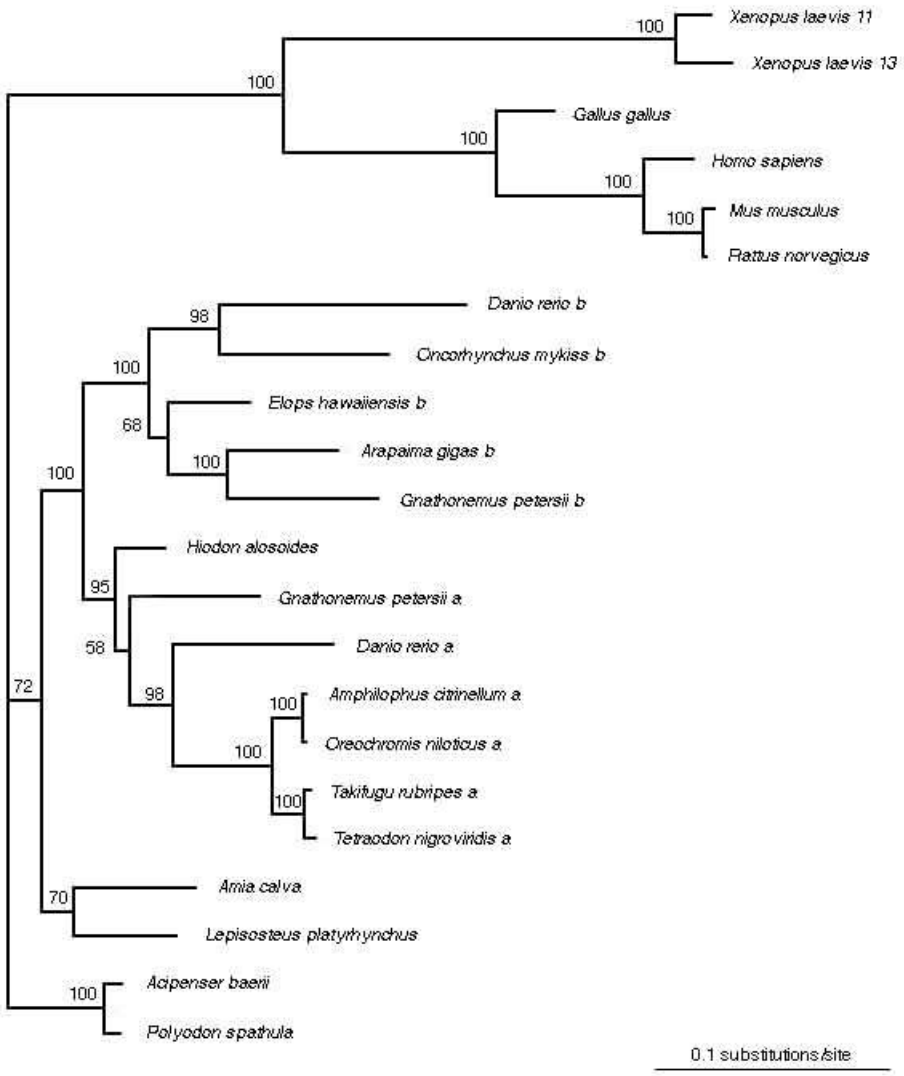

Supplementary figure 7. Bayesian tree derived from nucleotide sequences of nuclear gene data of first and second codon positions of *sox11*. The GTR+I+Γ model of sequence evolution was used. The values above the branches indicate Bayesian posterior probabilities.

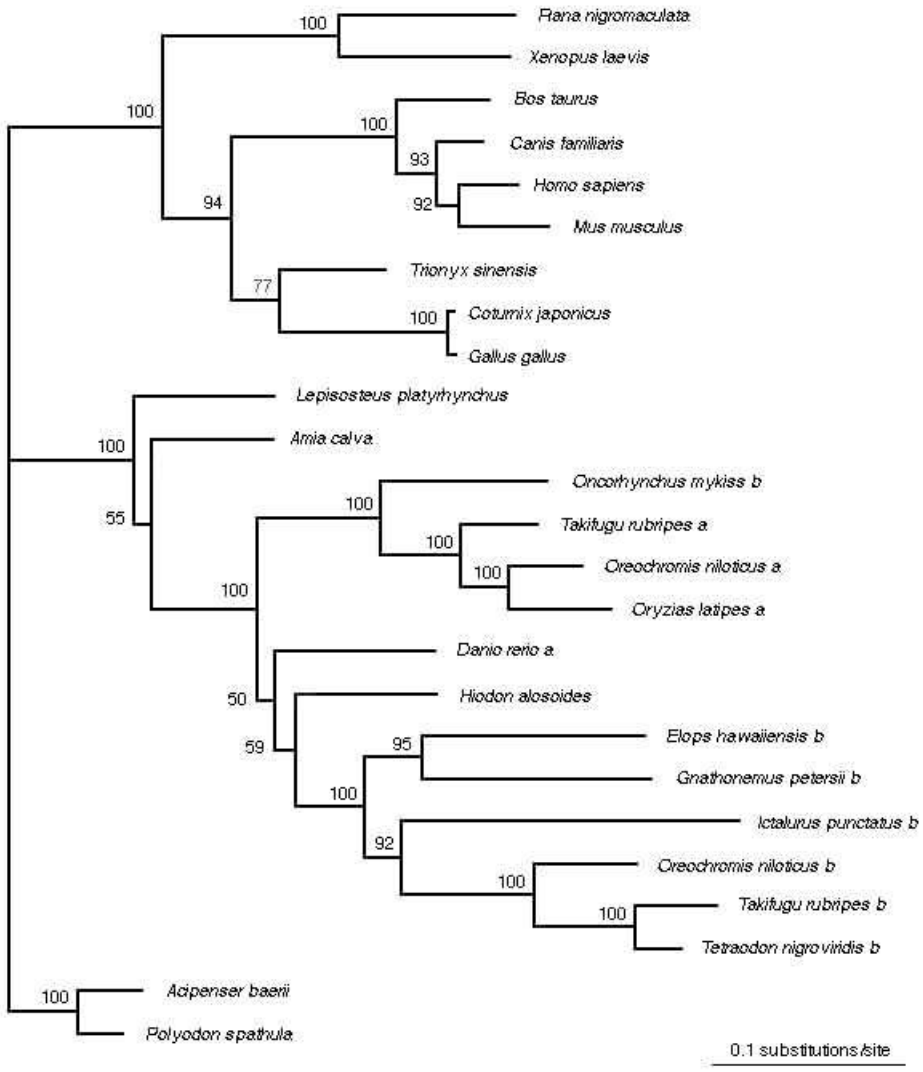

Supplementary figure 8. Bayesian tree derived from nucleotide sequences of nuclear gene data of first and second codon positions of *tyr*. The GTR+I+Γ model of sequence evolution was used. The values above the branches indicate Bayesian posterior probabilities.

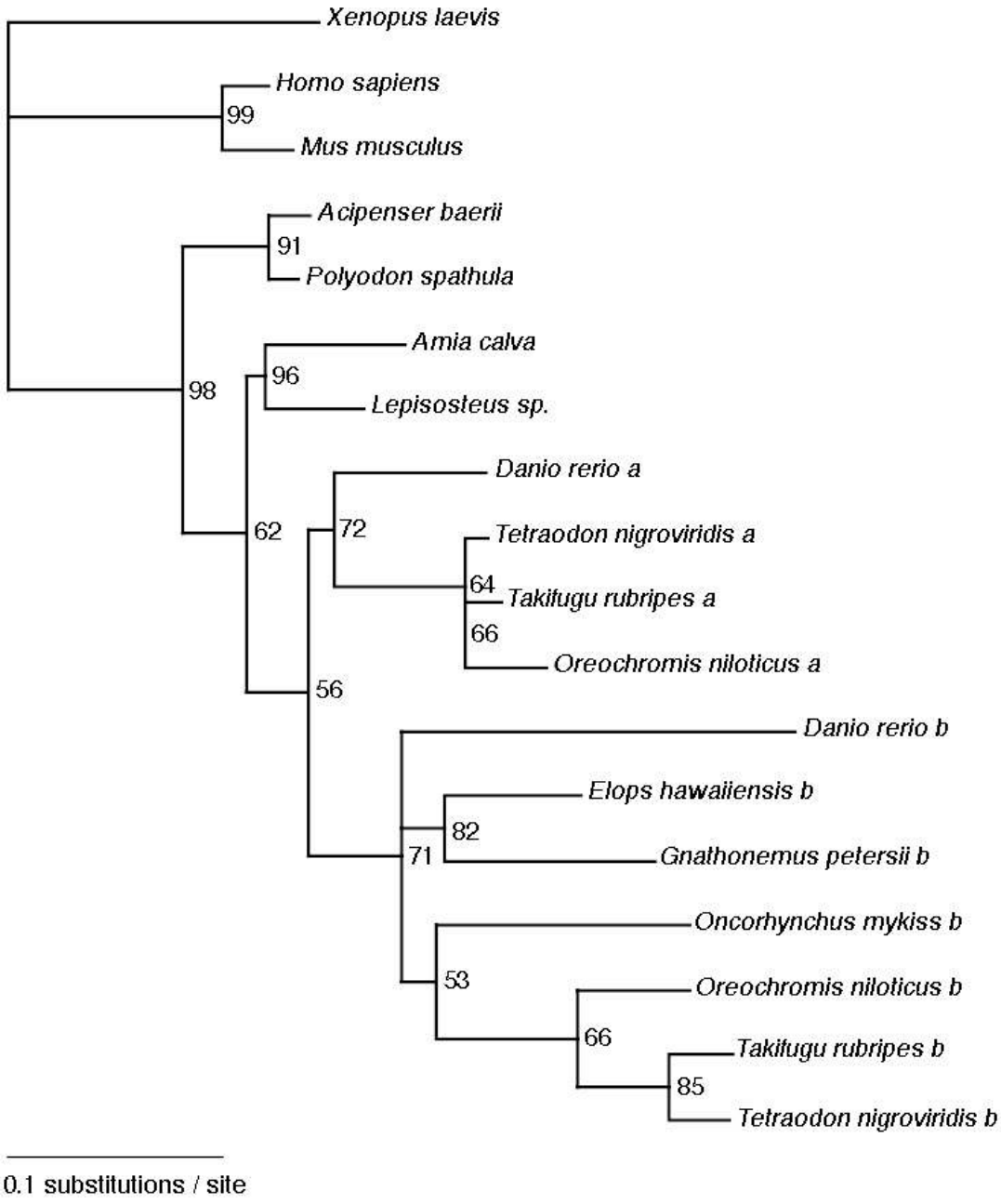

Supplementary figure 9. Phylogenetic relationships among actinopterygians inferred from Maximum Likelihood analysis of concatenated amino acid sequences of 4 nuclear genes (1260 amino acids) using the VT substitution model. Numbers on internal branches are measures of support derived from quartet puzzling.

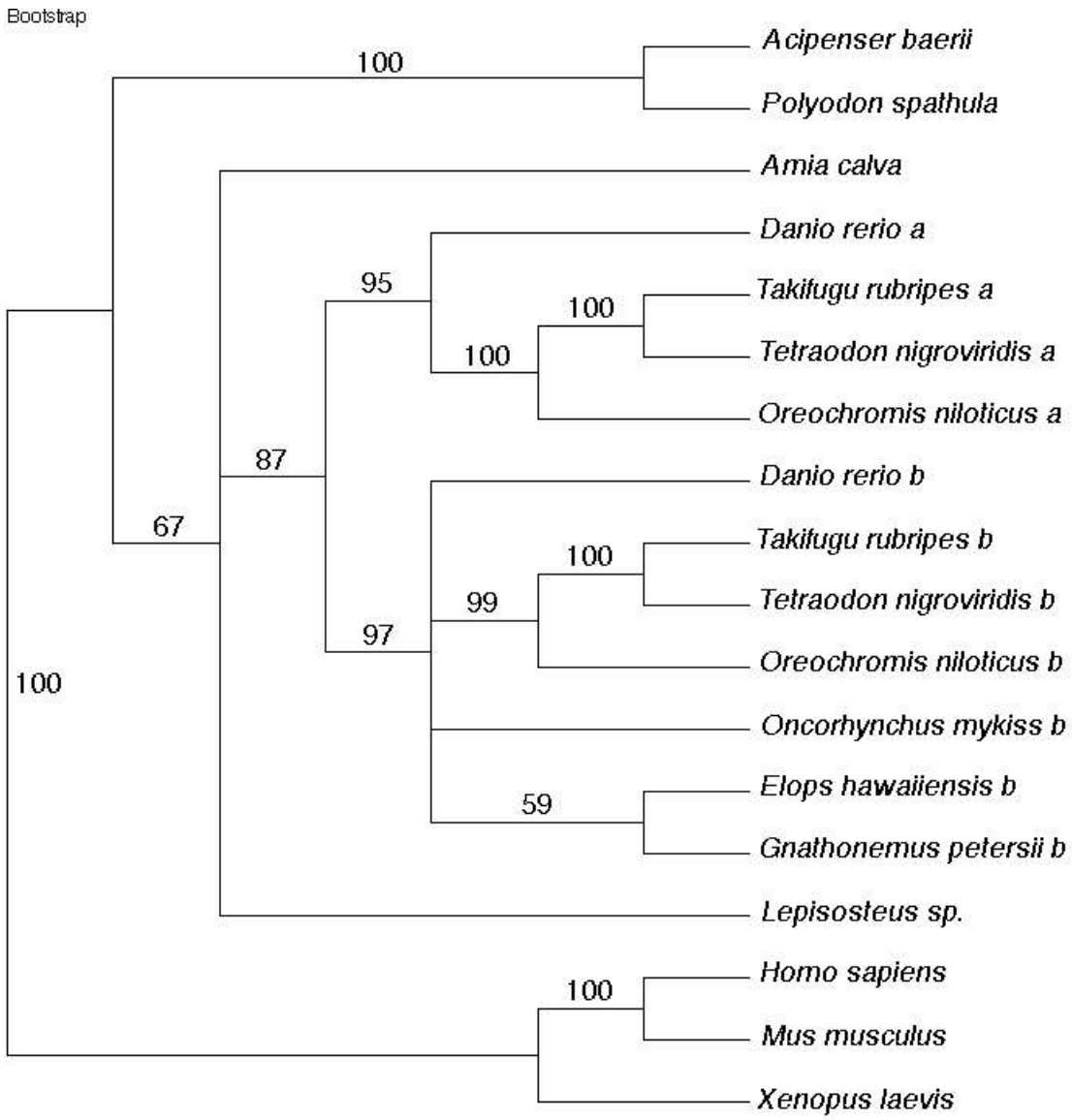

Supplementary figure 10. Phylogenetic relationships among actinopterygians inferred from Maximum Likelihood analysis of 2520 bp of concatenated nucleotide sequences of 4 nuclear genes (excluding third codon positions) using the GTR + I + Γ model of nucleotide substitution. Numbers on internal branches are Maximum Likelihood bootstrap proportions.

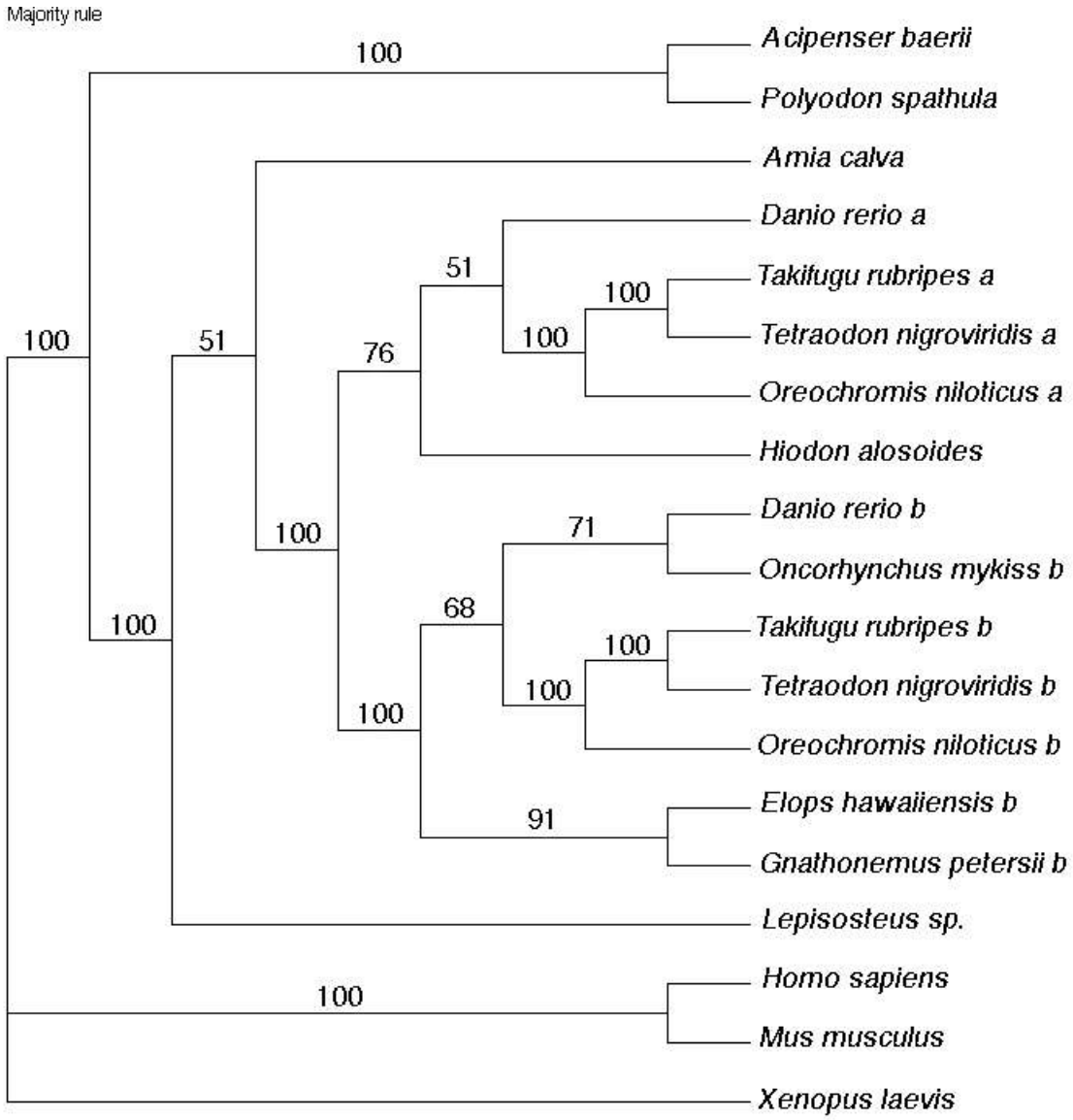

Supplemenary figure 11. Phylogenetic relationships among actinopterygians inferred from partitioned Bayesian analysis of 2520 bp of concatenated nucleotide sequences of 4 nuclear genes (excluding third codon positions) including *Hiodon alosoides* sequence. Numbers on internal branches are Bayesian posterior probabilities.

Supplementary figure 12. Maximum likelihood (ML) tree derived from nucleotide sequences of mitogenomic data of first and second codon positions of 11 protein coding genes (ND6 and ATPase 8 were excluded as well as third codon positions), and stem regions of 21 transfer RNA (tRNA) genes (Ser AGY and loops were excluded). The likelihood score was –ln L = 62082.62502. The GTR + I + Γ model of sequence evolution (Yang, 1994) was used. The same topology was obtained from a Bayesian analysis also based on the GTR + I + Γ model. The values above and below the branches indicate ML bootstrap support and Bayesian posterior probabilities respectively. Those branches without numbers had a value of 100%.

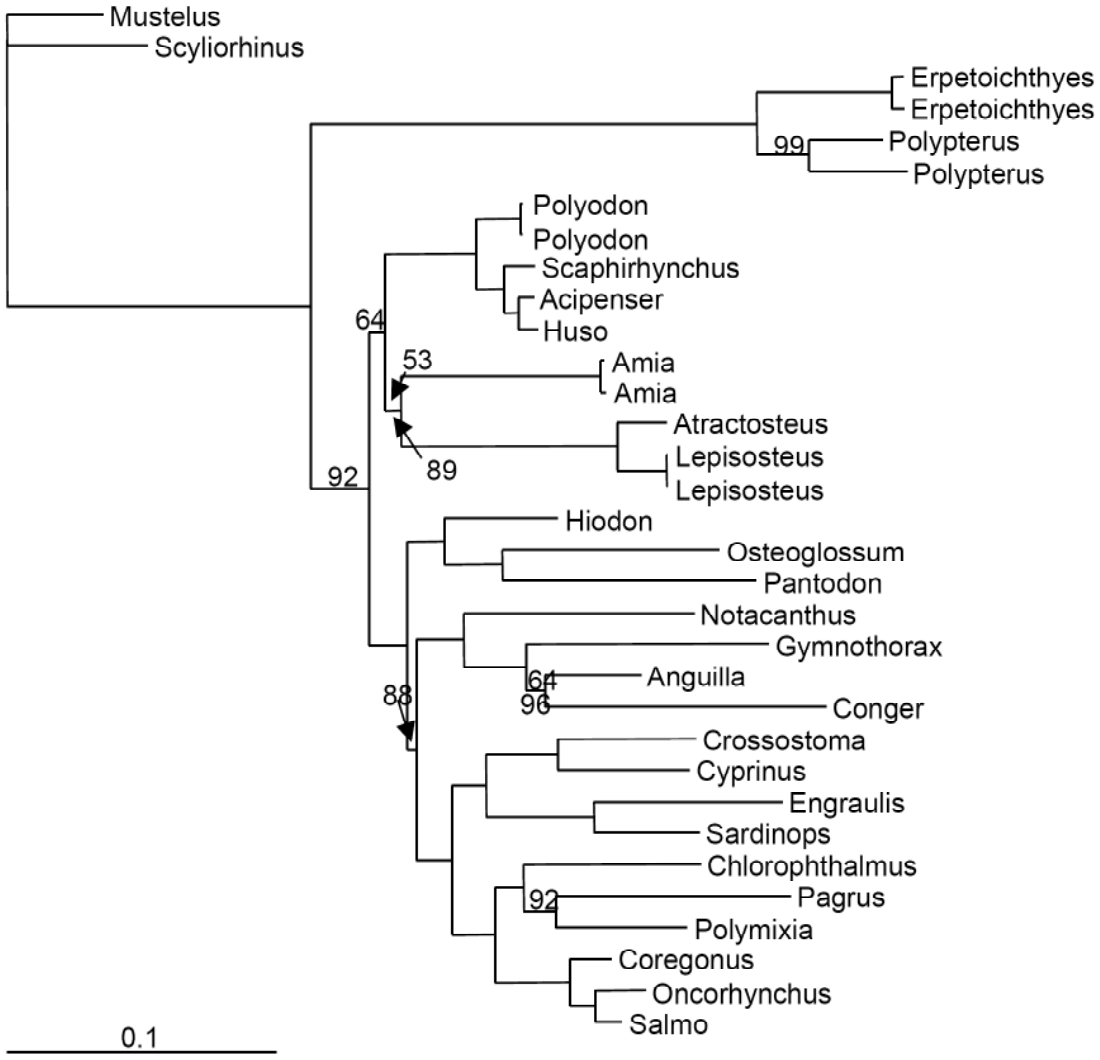

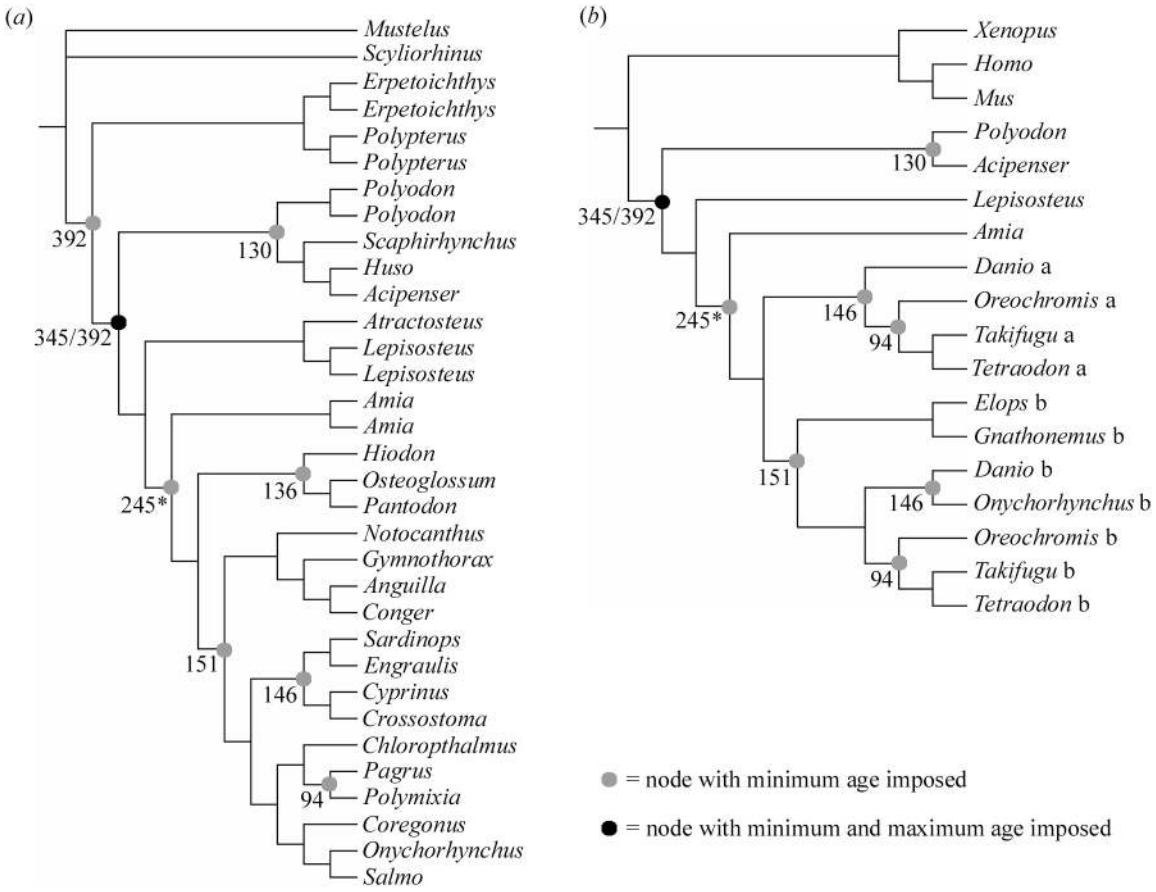

Supplementary figure 13. Fossil-based age constraints (Myr ago) used for Bayesian divergence date estimates (table 3). (*a*) constraints used in analysis of mitochondrial data; (*b*) constraints used in analysis of nuclear data. Nodes shown in grey have only a minimum age imposed, while those in black have both a maximum and minimum imposed. For full justification of these dates, consult Electronic supplementary material (*e*). The node marked with an asterisk refers to the divergence between *Amia* and its nearest living sister group. This date can be revised to 284 Myr ago based on the interpretation of the fossil genus *Brachydegma* presented here. Both topologies shown here reflect the halecostome branching pattern (*Lepisosteus* (*Amia* + Teleostei)), but in runs where the holostean branching pattern (Teleostei (*Lepisosteus* + *Amia*)) is enforced, this age constraint refers to the last common ancestor of *Amia* and *Lepisosteus*.